2019

Multi-proxy constraints on the significance of covariant δ13C values in carbonate and organic carbon during the early Mississippian

Amanda M. Oehlert

Peter K. Swart

Gregor P. Eberli

Samantha Evans

Tracy D. Frank

SEDIMENTOLOGY the journal of the International Association of Sedimentologists

Sedimentology (2019) **66**, 241–261 doi: 10.1111/sed.12502

Multi-proxy constraints on the significance of covariant $\delta^{13}C$ values in carbonate and organic carbon during the early Mississippian

AMANDA M. OEHLERT*, PETER K. SWART*, GREGOR P. EBERLI*, SAMANTHA EVANS† and TRACY D. FRANK‡

**Rosenstiel School of Marine and Atmospheric Sciences, 4600 Rickenbacker Causeway, Miami, FL, 33149, USA (E-mail: aoehlert@rsmas.miami.edu)*

†Boise State University, 1910 W University Dr, Boise, ID 83725, USA

‡University of Nebraska, 1400 R St, Lincoln, NE 68588, USA

Associate Editor – Stephen Lokier

ABSTRACT

This study investigates the covariation between carbonate and organic $\delta^{13}C$ values in a proximal to distal transect of four outcrops in the Madison Limestone in the Western United States Rockies, combined with $\delta^{34}S$ values of carbonate associated sulphate, the concentration of acid-insoluble material and measurements of total organic carbon. These new geochemical datasets not only allow for an evaluation of carbon isotope covariance during one of the largest perturbations to the global carbon cycle over the past 550 Myr, but also constrain the cause of the excursion in carbonate $\delta^{13}C$ values. The results support the hypothesis that a period of anoxia did not play a role in generating the positive carbonate $\delta^{13}C$ values, but rather favour interpretations by previous workers that the proliferation of land plants destabilized the Carboniferous carbon cycle, setting the stage for a significant change in the carbonate $\delta^{13}C$ values of contemporaneous marine carbonates. These results also demonstrate that one of the largest perturbations to the global carbon cycle did not produce synchronous variations in carbonate and organic $\delta^{13}C$ values, emphasizing the importance of local depositional controls on carbon isotope covariance in the geological record in both modern and ancient environments.

Keywords Carbonate, carbonate associated sulphate, Mississippian, organic carbon, stable isotopes.

INTRODUCTION

Perturbations to the global carbon cycle result in large changes in the $\delta^{13}C$ values of marine carbonates, and have often been linked to important biogeochemical events in Earth history, such as extinctions, periods of high productivity, evolutionary events and changes in the global redox conditions on Earth (Berner, 1994, 1998; Hayes *et al.*, 1999; Beerling & Berner, 2000; Berner & Kothvala, 2001; Berner, 2002; Saltzman *et al.*, 2004; Galli *et al.*, 2005; Immenhauser *et al.*, 2008; Jenkyns, 2010; Meyer *et al.*, 2013; and many others). In order to produce accurate interpretations of the dynamics of the ancient global carbon cycle, confidence in the primary, unaltered nature of the carbonate $\delta^{13}C$ values is fundamental. A positive correlation between coeval carbonate and organic $\delta^{13}C$ values from marine carbonates has been used as an indicator of pristine carbonate $\delta^{13}C$ values (Knoll *et al.*, 1986; Kaufman & Knoll, 1995; Hoffman *et al.*, 1998; Halverson *et al.*, 2002; Cramer & Saltzman, 2007; Young *et al.*, 2008; Luo *et al.*, 2010; Meyer *et al.*, 2013). This is based on the assumption that marine carbonates and organic material will equally record changes in the $\delta^{13}C$ values of the dissolved inorganic carbon (DIC) pool in the surface waters

of the ocean as it changes in response to perturbations in the global carbon cycle. Offset by photosynthetic fractionation, carbonate and organic $\delta^{13}C$ values are then assumed to record the response of the contemporaneous global carbon cycle in response to tectonic, volcanic, biogeochemical and weathering fluxes. This approach has been applied in a variety of studies of ancient deposits (Knoll *et al.*, 1986; Kaufman & Knoll, 1995; Hoffman *et al.*, 1998; Halverson *et al.*, 2002; Krull *et al.*, 2004; Werne & Hollander, 2004; Cramer & Saltzman, 2007; Young *et al.*, 2008; Ader *et al.*, 2009; LaPorte *et al.*, 2009; Nunn *et al.*, 2009; Korte & Kozur, 2010; Luo *et al.*, 2010; Swanson-Hysell *et al.*, 2010; Meyer *et al.*, 2011; Meyer *et al.*, 2013; Koevoets *et al.*, 2016; Caravaca *et al.*, 2017). In contrast, recent studies have found that diagenetic alteration, as well as syndepositional mixing between isotopically distinct sources of carbonate and organic matter, can produce highly covariant $\delta^{13}C$ values in marine carbonates and organic matter from a modern carbonate platform environment where age, diagenetic history, pCO_2, carbonate and organic matter producers, as well as sediment transport pathways, are well-constrained (Oehlert *et al.*, 2012; Oehlert & Swart, 2014). The results of these studies suggest that while carbon isotope covariance should be expected theoretically, local environmental factors can exert an overarching control in establishing the relationship between carbonate and organic $\delta^{13}C$ values in settings where multiple sources of carbonate and organic matter are contributed to a deposit.

In light of these observations, this study aims to evaluate the tipping point, where the overarching control on carbon isotope covariance may switch from local environmental factors to global carbon cycle dynamics, by investigating one of the largest positive excursions in carbonate $\delta^{13}C$ values during the Phanerozoic. This change is recorded in lowermost Carboniferous (Lower Mississippian) carbonates from the Ural Mountains (Saltzman *et al.*, 2004), the Dinant Basin in Belgium (Saltzman *et al.*, 2004) and multiple locations in the western United States (Bruckschen *et al.*, 1999; Mii *et al.*, 1999; Saltzman, 2002, 2003; Gill *et al.*, 2007; Koch *et al.*, 2014), including the transect of four outcrops studied here (Fig. 1; Katz *et al.*, 2007), each of which record peak carbonate $\delta^{13}C$ values $\geq +7‰$ in the western US (Saltzman *et al.*, 2004). The globally recognizable positive excursion in carbonate $\delta^{13}C$ values occurs in Sequence II of the Lodgepole Formation within the Madison Limestone at the boundary between the Kinderhookian and Osagean stages 355·5 Ma (Fig. 2; Sando, 1985; Elrick & Read, 1991; Saltzman *et al.*, 2000; Saltzman *et al.*, 2004; Buoniconti, 2008). Understanding the cause of this large positive excursion in carbonate $\delta^{13}C$ values has been a focus of many recent studies because it occurs during a period of intense change in Earth history, including a transition from greenhouse to icehouse conditions (Crowell, 1999) and the general concurrence with the evolution of vascular land plants (Berner, 1998; Berner & Petsch, 1998). Such transient anomalies in carbonate $\delta^{13}C$ values can be difficult to model (Saltzman *et al.*, 2004) and can occur as a result of processes unrelated to global carbon cycling (Swart & Eberli, 2005; Swart, 2008). These difficulties are especially apparent in ancient epeiric seaways where local processes can overprint or exaggerate global carbon cycling signatures (Immenhauser *et al.*, 2003, 2008). As a result, previous studies aiming to constrain the initiation of this large positive excursion in carbonate $\delta^{13}C$ values alone have presented conflicting interpretations. Proposed mechanisms have included the enhanced sequestration of carbon in terrestrial sinks as a result of the evolution of vascular land plants (Berner, 1998), the weathering of ancient uplifted carbonates (Saltzman, 2003) and a major increase in productivity resulting from a large marine transgression (Katz *et al.*, 2007). Tectonic forcings, such as uplifts in the mid-latitudes and subsequent reduction in Earth's surface temperatures and pCO_2 resulting from increased albedo (Veevers & Powell, 1987) and the low-latitude Antler Orogeny, which may have enhanced rates of organic carbon burial as a result of increased flysch deposition (Saltzman *et al.*, 2000; Saltzman, 2003) have also been proposed. The variability in mechanisms proposed suggests that further investigation with additional geochemical constraints is necessary, which will improve understanding of the hierarchical control of intrinsic and extrinsic controls on carbon isotope covariance.

In this study, the relationship between the $\delta^{13}C$ values of carbonate and organic matter is evaluated in a proximal to distal transect of outcrops of the *ca* 350 Myr Madison Limestone (Freemont Canyon, Wind River Canyon, Sheep Mountain and Benbow Mine Road; Fig. 1) during one of the most significant perturbations to the Phanerozoic global carbon cycle. A multiproxy geochemical approach is employed in order to evaluate the lack of covariance between carbonate and organic $\delta^{13}C$ values, and to constrain the mechanism for this perturbation.

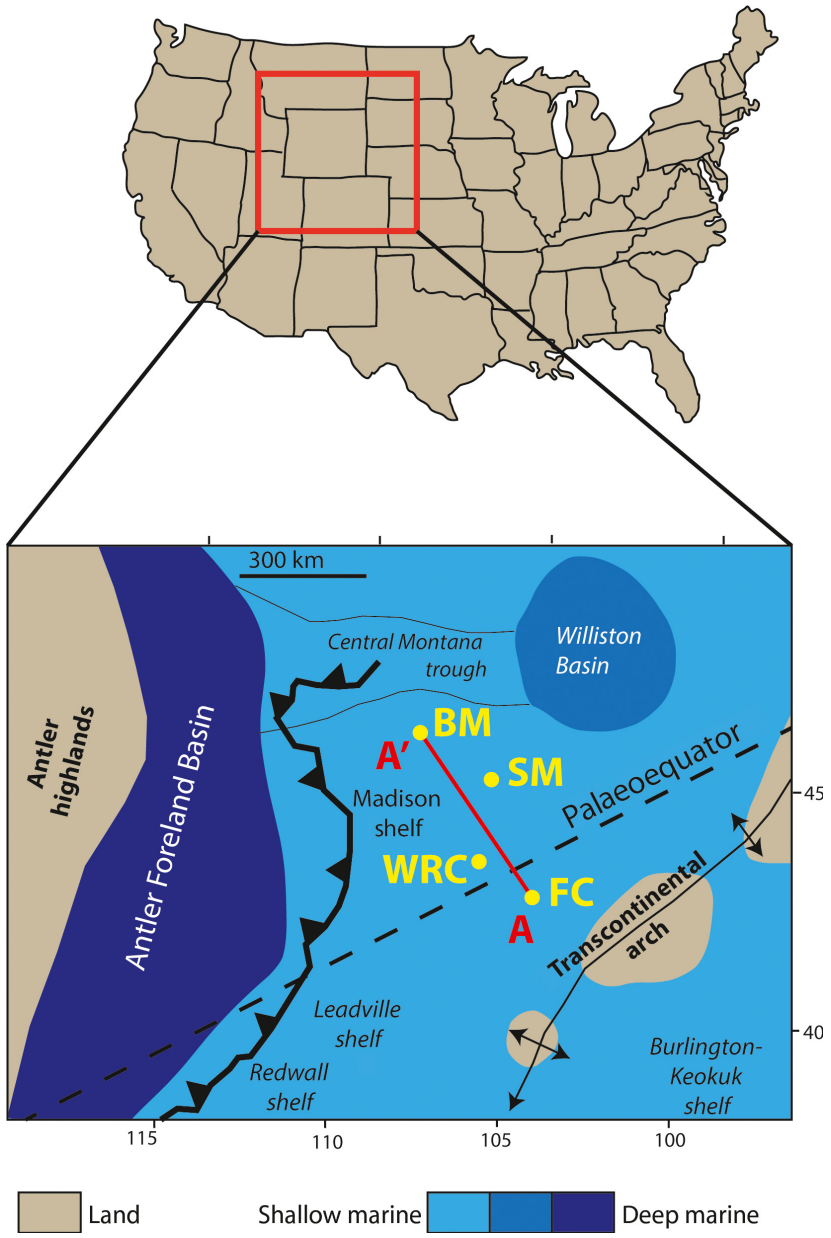

Fig. 1. Palaeogeographic map of the Madison Limestone and study locations: Freemont Canyon (FC; 42°29′31.5″N, 106°46′47.5″W); Wind River Canyon (WRC; 43°31′52″N, 108°10′40.5″W); Sheep Mountain (SM; 44°36′40.1″N, 108°8′23.2″W) and Benbow Mine Road (BM; 45°22′25.3″N, 109°47′39.3″W). Modified from Gutschick & Sandberg (1983), Sonnenfeld (1996) and Katz *et al.* (2007). Red line labelled A–A' is the same line as shown in Fig. 3.

GEOLOGICAL SETTING

The mostly Lower Mississippian Madison Limestone is an extensive carbonate ramp extending from the Canadian Arctic to New Mexico (Maughan, 1983; Scotese & McKerrow, 1990). The Madison Limestone was deposited within 0 to 10°N of the palaeoequator and had an extent of more than 640 000 km^2 (Maughan, 1983; Scotese & McKerrow, 1990; Katz *et al.*, 2007). Outcrops occur in Montana, Wyoming and Nevada (Sando, 1985; Katz *et al.*, 2007; Buoniconti, 2008), and regional equivalents have also been mapped in the mid-continent, in Iowa, Illinois, Indiana, Missouri, Oklahoma and Texas (Mii *et al.*, 1999), as well as in drill cores from Kansas, Nebraska, Iowa, Missouri and Oklahoma (Mii *et al.*, 1999; Koch *et al.*, 2014). The Madison shelf was bounded by the Transcontinental Arch to the east, and deepened to the west into the Antler Trough and into the Montana Trough and Williston Basin to the north (Sando, 1977, 1985; Gutschick *et al.*, 1980; Maughan, 1983; Smith *et al.*, 2004; Buoniconti, 2008).

The Madison Limestone was deposited on a gently dipping ramp with laterally extensive,

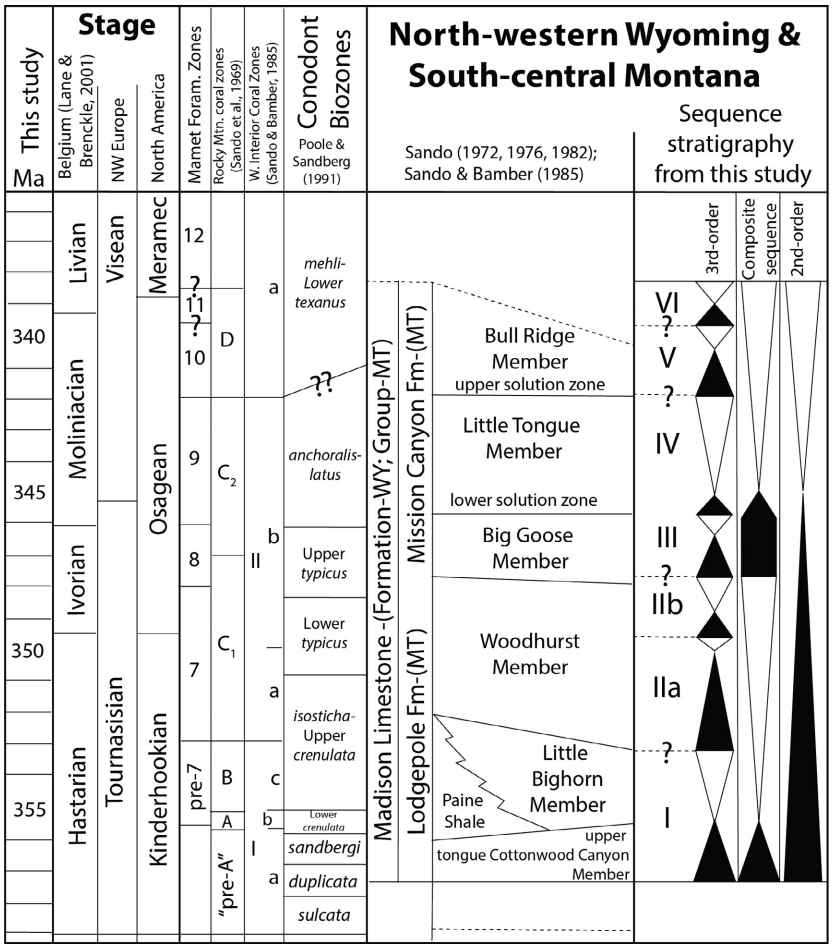

Fig. 2. Chronostratigraphic chart of the Madison Limestone depositional sequences (modified from Sonnenfeld, 1996; Katz *et al.*, 2007). Within the sequence stratigraphy from Katz (2008) black triangles represent transgressive hemicycles while white triangles are the regressive hemicycles. Madison Limestone biostratigraphy was based on the correlation of Rocky Mountain megafauna and Mamet Foram Zones (Sando *et al.*, 1969; Sando & Bamber, 1985). Stage boundaries were correlated to the Gradstein *et al.* (2004) timescale for North America and NW Europe. Lane & Brenckle (2001) stages from Belgium are also shown. Dates between stage boundaries were adjusted through comparison of $^{87}Sr/^{86}Sr$ analysis of Sheep Mountain and Sacagawea Peak samples with the seawater $^{87}Sr/^{86}Sr$ curve (Bruckschen *et al.*, 1999; Mii *et al.*, 1999).

uniform facies belts that can reach 100 km of width (Elrick & Read, 1991; Sonnenfeld, 1996; Smith *et al.*, 2004; Westphal *et al.*, 2004; Buoniconti, 2008). The shallow-water deposits are mostly comprised of dolomite and limestones, but the base of the formation and the more basinward sections of the ramp are more argillaceous (Sonnenfeld, 1996; Smith *et al.*, 2004; Westphal *et al.*, 2004; Katz *et al.*, 2007). High-frequency sea-level fluctuations forced facies belts to shift on the ramp. As a result, facies belts stepped landward during transgressions and prograded seaward during regressions (Sonnenfeld, 1996). The entire Madison Limestone represents one second-order supersequence that internally consists of six third-order sequences (Sonnenfeld, 1996; Smith *et al.*, 2004; Westphal *et al.*, 2004). This study focuses on the three oldest third-order sequences, I, II and III, which comprise the Lodgepole Formation and the bottom of the Mission Canyon Formation (Sando, 1977, 1985; Gutschick *et al.*, 1980; Sonnenfeld, 1996; Smith *et al.*, 2004; Buoniconti, 2008).

PREVIOUS WORK ON DOLOMITE IN THE MADISON LIMESTONE

The Madison Limestone is in certain places heavily dolomitized and the distribution of the dolomite largely follows a sequence stratigraphic framework (Smith *et al.*, 2004; Katz *et al.*, 2007; Katz, 2008). Based on thin section photomicrographs, Smith *et al.* (2004) deciphered a paragenetic sequence that includes early syndepositional dolomite to later burial dolomitization (Smith *et al.*, 2004, fig. 10). Dolomite morphology includes early/syndepositional dolomite rhombs, dolomitic mudstones, dolomitized grainstones with a sucrosic texture, to coarser, early burial dolomite (Smith *et al.*, 2004 – photomicrographs of fabrics shown in figs 11 and 12). The amount of dolomitization varies along the ramp and vertically within each section. Fabric selective dolomitization is common in the down-dip areas of the ramp with mud-dominated strata, where more than 90% of mud-rich intervals were dolomitized,

while <5% of the grain-dominated intervals were dolomitized (Smith *et al.*, 2004). The mud-rich intervals are part of the transgressive hemicycles while the grain-dominated strata constitute the regressive portion of each depositional cycle. In the middle ramp sections, dolomitization is pervasive in the transgressive portion of the second-order supersequence (Sequences I to III) where both the mud-dominated and grain-dominated facies are dolomitized. The regressive portion of the supersequence (Sequence IV), however, is a limestone. Towards the up-dip part of the Madison ramp, dolomitization is 'patchy' but again the transgressive intervals are more dolomitized (Smith *et al.*, 2004). Although the mineralogy in the Madison Limestone varies along the ramp from alternating limestone–dolomite to pervasive dolomite, the magnitude and expression of the positive shift in carbonate $\delta^{13}C$ values was found to be independent of mineralogy and facies (Katz *et al.*, 2007).

MATERIALS AND METHODS

Samples

The analyzed samples were collected from four outcrops of the Madison Limestone, including exposures in Freemont Canyon, Wind River Canyon, Sheep Mountain and the Benbow Mine Road outcrops (Fig. 1; Smith *et al.*, 2004; Katz *et al.*, 2007; Buoniconti, 2008). The $\delta^{13}C$ values of the bulk carbonates, consisting of both calcite and dolomite, from these outcrops have been reported previously (Katz *et al.*, 2007), and geochemical and isotopic analyses reported in this study used the same samples.

Organic $\delta^{13}C$ values and acid-insoluble material

Co-occurring sedimentary organic matter was separated via dissolution in 10% HCl acid following the method described in Oehlert *et al.* (2012). Samples were analyzed using a Costech ECS 4010 (Costech Analytical Technologies Inc., Valencia, CA, USA). The resulting CO_2 gas was transferred for isotopic measurement to a continuous flow isotope-ratio mass spectrometer (Delta V Advantage; Thermo Fisher Scientific, Waltham, MA, USA). The reproducibility of $\delta^{13}C$ values is $\pm 0{\cdot}1‰$ as indicated by the standard deviation of replicate analyses of internal standards of glycine [$n = 54$; $\delta^{13}C_{org}$ value = $-31{\cdot}8‰$ Vienna Pee Dee Belemnite (VPDB)]. All $\delta^{13}C_{org}$ data are reported relative to the VPDB scale, defined for organic carbon as the $\delta^{13}C$ value of graphite (USGS24) = $-16{\cdot}05‰$ versus VPDB (Coplen *et al.*, 2006).

Insoluble residue and total organic carbon

Weights and percentages of insoluble residue and total organic carbon (TOC) were analyzed and calculated following the methods of Oehlert *et al.* (2012). The standard deviation of these analyses is 0·4% based upon repeated analyses of glycine ($n = 54$).

Carbonate associated sulphate

Samples analyzed for $\delta^{34}S_{CAS}$ values were prepared following the methodology of Gill *et al.* (2011). Samples were combusted using a Dumas type combustion system (Europa Scientific, Crewe, UK) and the resultant SO_2 gas was analyzed using a continuous flow isotope-ratio mass spectrometer (CFIRMS 20-20; Europa Scientific). Variations in ^{18}O were eliminated by passing the SO_2 over quartz at 1000°C (Fry *et al.*, 2002). Data are reported in ‰ relative to Vienna Canyon Diablo Troilite (V-CDT) using the conventional notation. Reproducibility of measurements was assessed from repeated analyses of standards of known weight and composition, and the average standard error for all three standards is $0{\cdot}2‰$ based on 86 replicate analyses.

Carbonate mineralogy

The carbonate mineralogy was determined using a PANalytical X'pert X-ray Diffractometer (PANalytical Inc, Almelo, The Netherlands). Samples were powdered using a mortar and pestle, and spread onto a glass slide. Samples were allowed to air dry overnight before analysis. The proportions of low-magnesium calcite (LMC) and dolomite were calculated from a model that assumes that the sample is entirely composed of aragonite, LMC and dolomite. Based upon eleven replicate analyses of the same sample, the standard error of the analysis is *ca* 3%.

RESULTS

Organic $\delta^{13}C$ values

The $\delta^{13}C$ values of organic matter from the four Madison Limestone outcrops range from $-20{\cdot}1$

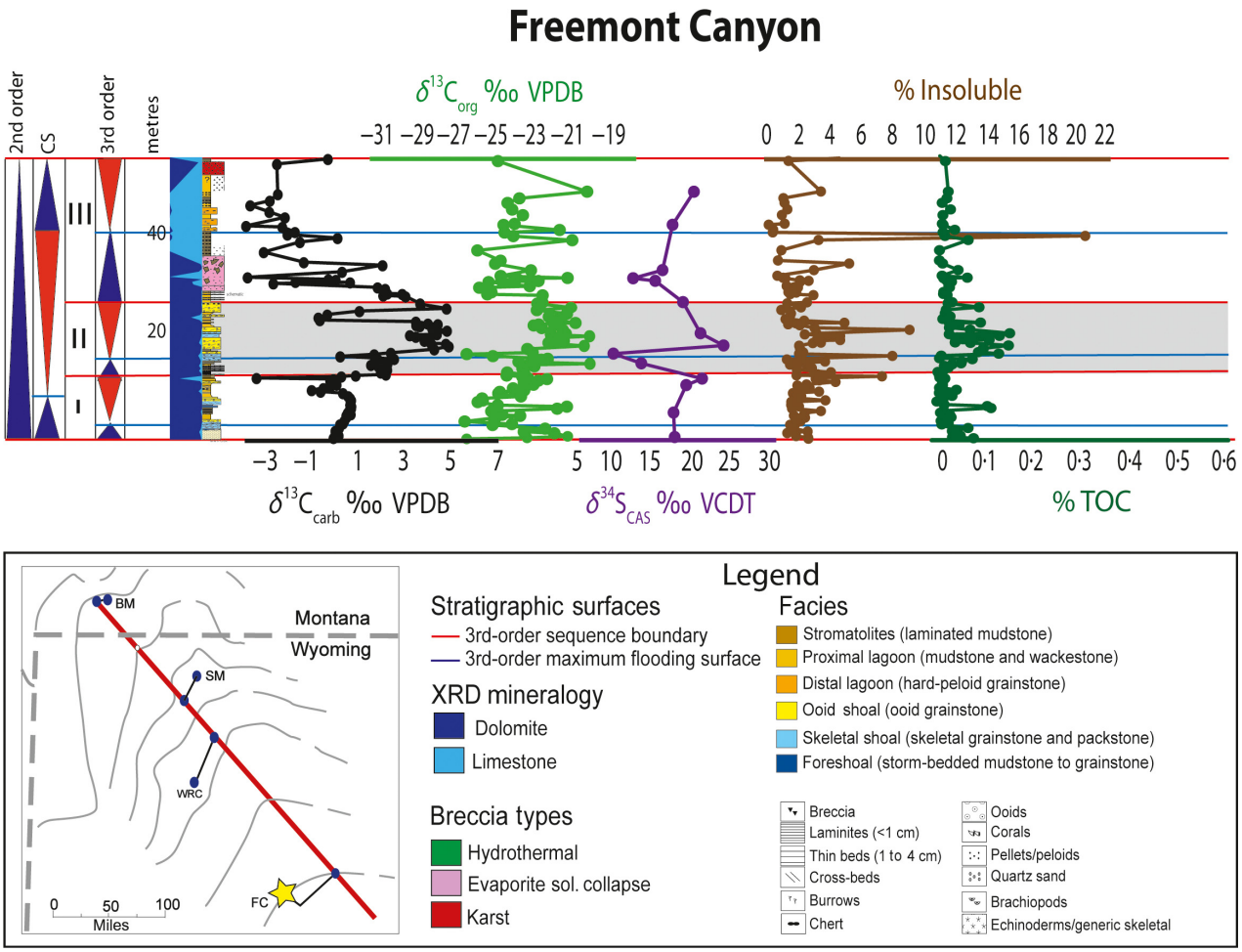

Fig. 3. Stratigraphic plots of geochemical records from Freemont Canyon (FC; 42°29′31.5″N, 106°46′47.5″W), including carbonate mineralogy, carbonate $\delta^{13}C$ values (from Katz *et al.*, 2007), organic $\delta^{13}C$ values, $\delta^{34}S_{CAS}$ values, % acid insoluble material and % total organic carbon (TOC). Sequence stratigraphy and sedimentological descriptions from Smith *et al.* (2004). In the map of outcrop locations, the red line denotes the same transect as presented in Fig. 1 and the yellow star indicates the outcrop from which the data presented in this figure were collected. CS, Cycle Sets; BM, Benbow Mine; SM, Sheep Mountain; VCDT, Vienna Canyon Diablo Troilite; VPDB, Vienna Pee Dee Belemnite; WRC, Wind River Canyon.

to −31·1‰ (Figs 3 to 6). Average values decrease with increasing distance from the Transcontinental Arch (Table 1). The average organic $\delta^{13}C$ values are highest in Sequence II at each of the four outcrops, while $\delta^{13}C$ values from Sequence I are the lowest (Table 1). Baseline values for pre-excursion organic $\delta^{13}C$ values range from −26‰ at Freemont Canyon and Wind River Canyon, to −28‰ at Sheep Mountain and Benbow Mine Road (Figs 3 to 6). Maximum values occurring during Sequence II also exhibit a spatial trend (Figs 3 to 6), where the most positive values were observed in the proximal locations of Freemont Canyon (−20‰) and Wind River Canyon (−21‰), to lower maximum organic $\delta^{13}C$ values at the distal locations of Sheep Mountain (−22‰) and Benbow Mine Road (−23‰). The difference between the maximum observed values in Sequence II and the average baseline value from Sequence I for each outcrop is consistently 6‰.

Correlation between carbonate and organic $\delta^{13}C$ values

Generally, the correlation between carbonate and organic $\delta^{13}C$ values is low at each of the outcrop locations when the records from Sequences I, II and III are combined (Table 2; Fig. 7), with the highest correlation observed at Sheep Mountain ($r^2 = 0{\cdot}25$, $P < 0{\cdot}05$, $n = 224$).

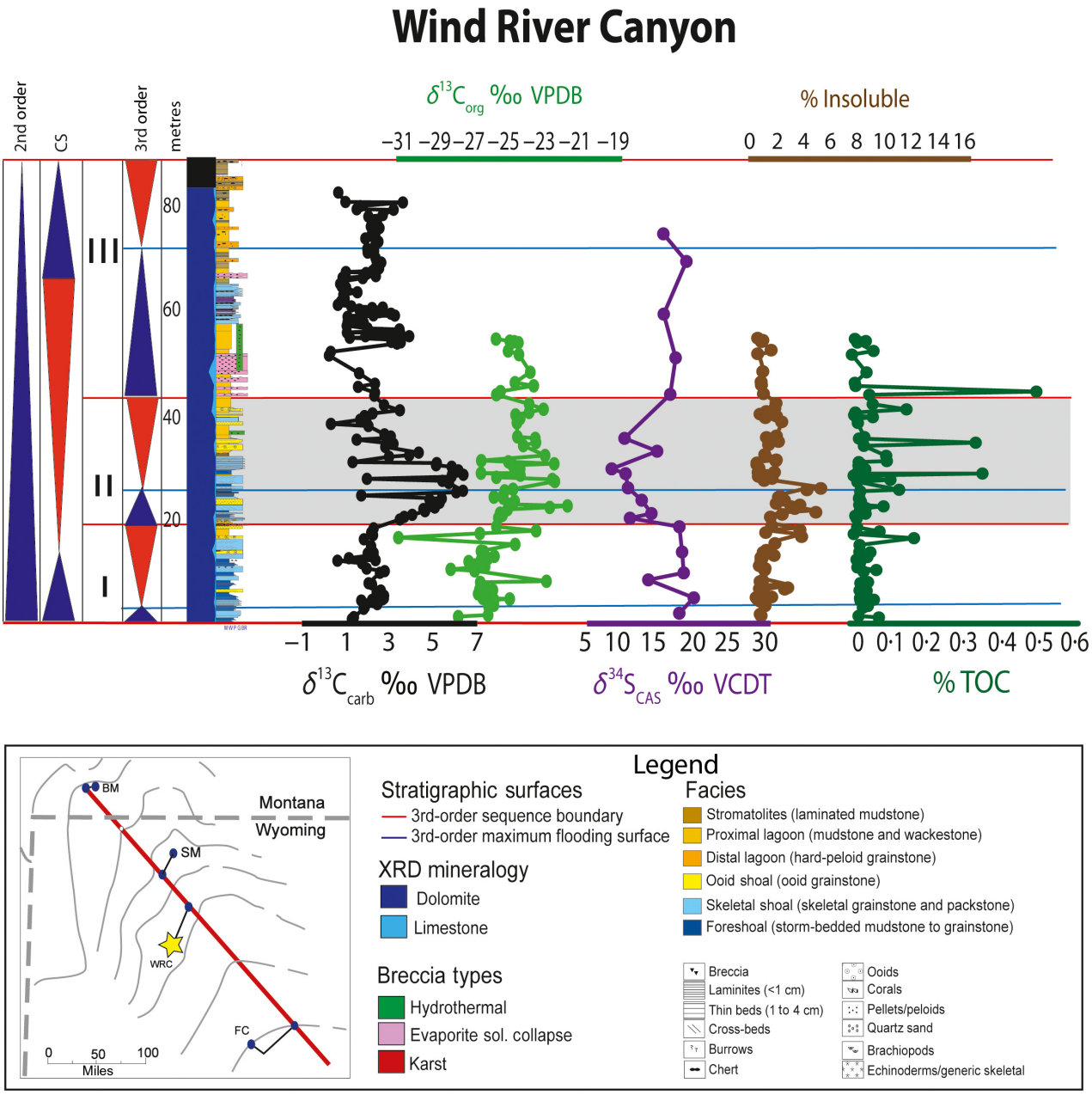

Fig. 4. Stratigraphic plots of geochemical records from Wind River Canyon (WRC; 43°31′52″N, 108°10′40.5″W), including carbonate mineralogy, carbonate $\delta^{13}C$ values (from Katz *et al.*, 2007), organic $\delta^{13}C$ values, $\delta^{34}S_{CAS}$ values, % acid insoluble material and % total organic carbon (TOC). Sequence stratigraphy and sedimentological descriptions from Smith *et al.* (2004). In the map of outcrop locations, the red line denotes the same transect as presented in Fig. 1 and the yellow star indicates the outcrop from which the data presented in this figure were collected. CS, Cycle Sets; BM, Benbow Mine; FC, Freemont Canyon; SM, Sheep Mountain; VCDT, Vienna Canyon Diablo Troilite; VPDB, Vienna Pee Dee Belemnite.

Separating the records by sequence shows higher correlation between carbonate and organic $\delta^{13}C$ values in Sequence II (Table 2; Figs 3 to 6). Within Sequence II, the correlation between carbonate and organic $\delta^{13}C$ values becomes stronger with increasing distance from the Transcontinental Arch (Table 2; Figs 3 to 6).

Total organic carbon

Total organic carbon (TOC) was measured at Benbow Mine Road, Wind River Canyon and Freemont Canyon, and average values are listed in Table 1. Significant peaks in the concentration of TOC are observed in the distal portion of the Madison

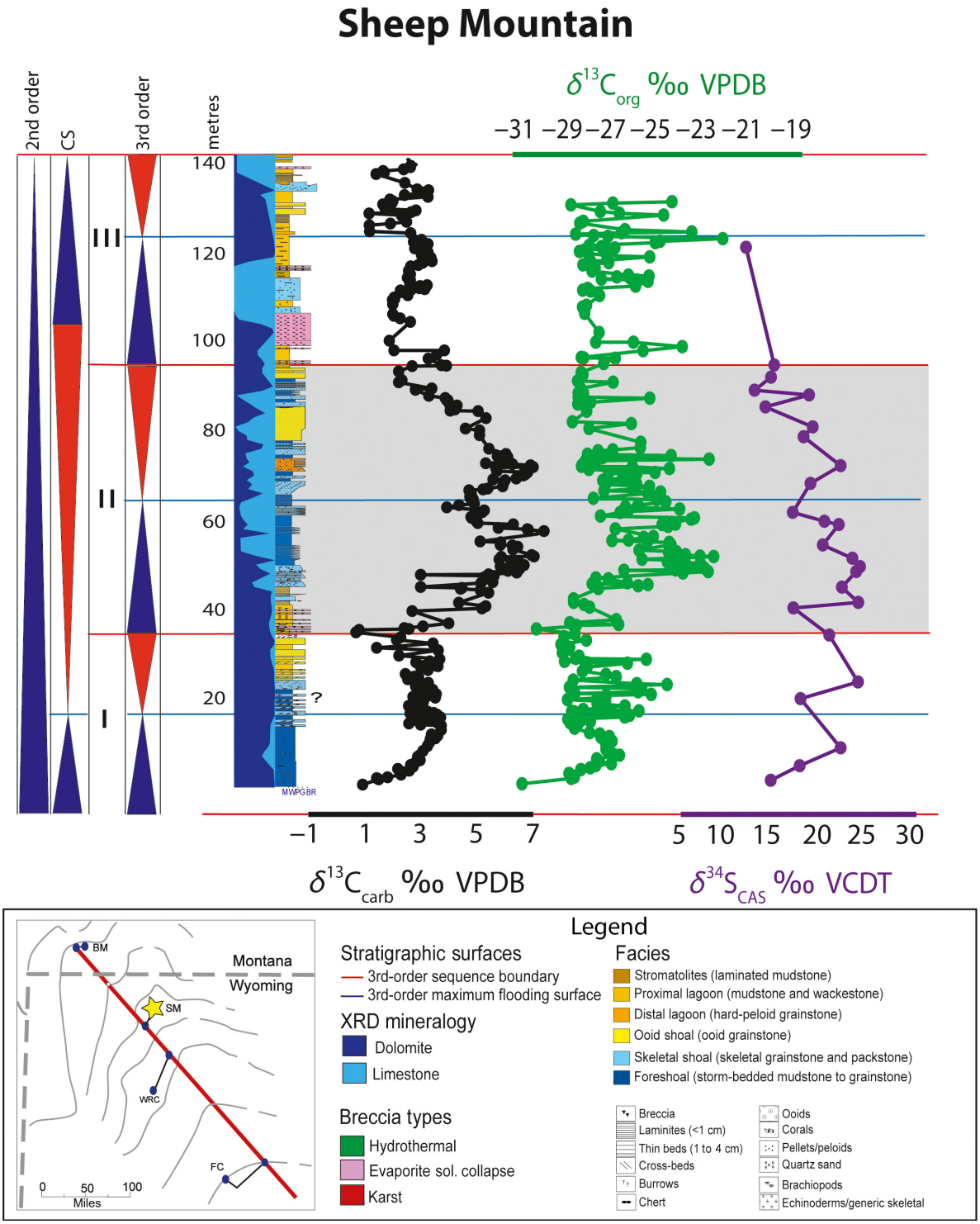

Fig. 5. Stratigraphic plots of geochemical records from Sheep Mountain (SM; 44°36′40.1″N, 108°8′23.2″W), including carbonate mineralogy, carbonate $\delta^{13}C$ values (from Katz *et al.*, 2007), organic $\delta^{13}C$ values, $\delta^{34}S_{CAS}$ values, % acid insoluble material and % total organic carbon (TOC). Sequence stratigraphy and sedimentological descriptions from Smith *et al.* (2004). In the map of outcrop locations, the red line denotes the same transect as presented in Fig. 1 and the yellow star indicates the outcrop from which the data presented in this figure were collected. CS, Cycle Sets; BM, Benbow Mine; FC, Freemont Canyon; VCDT, Vienna Canyon Diablo Troilite; VPDB, Vienna Pee Dee Belemnite; WRC, Wind River Canyon.

Limestone at Benbow Mine Road in Sequence I (0·5%), as well as a peak of 0·49% at Wind River Canyon within Sequence II (Figs 3, 4 and 6).

Acid-insoluble material

Acid-insoluble material was analyzed as a proxy for siliciclastic input to the system. The percentage of insoluble residue (%IR) was measured on samples collected from Benbow Mine Road, Wind River Canyon and Freemont Canyon, and average concentrations are listed in Table 1. The concentration of insoluble material ranges from a minimum value of 0·2 wt% to a maximum value of 21·3 wt%. The peak concentrations of %IR measured in Sequence II occurs at Benbow Mine Road, with a maximum value of 15·0% but the highest %IR measured within the Madison transect (21·3%) occurs within Sequence III at the most proximal location, Freemont Canyon.

Sulphur isotopes of carbonate associated sulphate

Records of $\delta^{34}S_{CAS}$ values were measured in all four locations and a proximal to distal trend of increasing average $\delta^{34}S_{CAS}$ values is observed within the transect (Table 1; Figs 3 to 6). General trends of increasing $\delta^{34}S_{CAS}$ values within Sequence II occur at Benbow Mine Road and Sheep Mountain (Figs 4 and 5). In contrast, $\delta^{34}S_{CAS}$ values from Wind River Canyon exhibit a marked decrease within Sequence II (Fig. 4), while $\delta^{34}S_{CAS}$ values from Freemont Canyon exhibit a decreasing trend below the maximum flooding surface (mfs), above which the $\delta^{34}S_{CAS}$ values change dramatically to more positive values (Fig. 3).

Correlations between all geochemical records

The relationships between each geochemical record [$\delta^{34}S_{CAS}$, carbonate and organic $\delta^{13}C$ values, TOC, concentration of acid insoluble materials and carbonate associated sulphate, along with published carbonate $\delta^{13}C$ values (Katz *et al.*, 2007)], were assessed using Pearson's regression analysis, and the correlation coefficient (r^2) is listed for each outcrop in Table 2. Statistically significant correlations are listed in bold text in Table 2.

Concentration of carbonate associated sulphate

The average concentration of CAS at each outcrop exhibits an increasing trend with distance from the palaeoshoreline and average values for each outcrop are listed in Table 1.

Carbonate mineralogy

On average, dolomite, as identified by X-ray diffractometry, was the predominant carbonate mineral measured at each outcrop. The average proportion of dolomite was, however, variable with higher average proportions occurring in the proximal outcrops Wind River Canyon (97%) and Freemont Canyon (81%) when compared to the average proportion of dolomite at the distal outcrops Sheep Mountain (57%) and Benbow Mine Road (70%). When the records are divided by sequence, some trans-ramp trends become apparent. The sequence with the lowest average proportion of dolomite is Sequence III, where calcite is the predominant mineralogy at Sheep Mountain (54%). In contrast, the highest average proportion of dolomite occurs in Sequence I across the Madison Transect (Table 1). Sequence II exhibits the most variable proportions of dolomite along the transect (Table 1; Figs 2 to 5), with proportions of dolomite being the highest at Wind River Canyon (96%) and the lowest at Sheep Mountain (45%; Table 1).

DISCUSSION

Carbonate $\delta^{13}C$ values record a global change in the Lower Mississippian carbon cycle

Based upon published studies of age equivalent sections, the excursion in bulk carbonate $\delta^{13}C$ values in the Madison Formation is likely to be an original record of contemporaneous marine DIC, rather than local or diagenetic effects, because it is observed globally (Bruckschen *et al.*, 1999; Mii *et al.*, 1999; Saltzman, 2002, 2003; Saltzman *et al.*, 2004; Gill *et al.*, 2007; Koch *et al.*, 2014) and the change occurs independently of facies (Katz, 2008). Furthermore, analysis of both calcite and dolomite minerals in the deposit show the same trends (Katz *et al.*, 2007) suggesting that the shift in bulk $\delta^{13}C$ values in marine carbonates was not driven by diagenesis. In the following discussion, the bulk carbonate $\delta^{13}C$ values published in Katz *et al.* (2007) will be compared with the records of organic $\delta^{13}C$ values, $\delta^{34}S_{CAS}$, TOC, acid-insoluble residue, mineralogy and concentrations of CAS measured in this study.

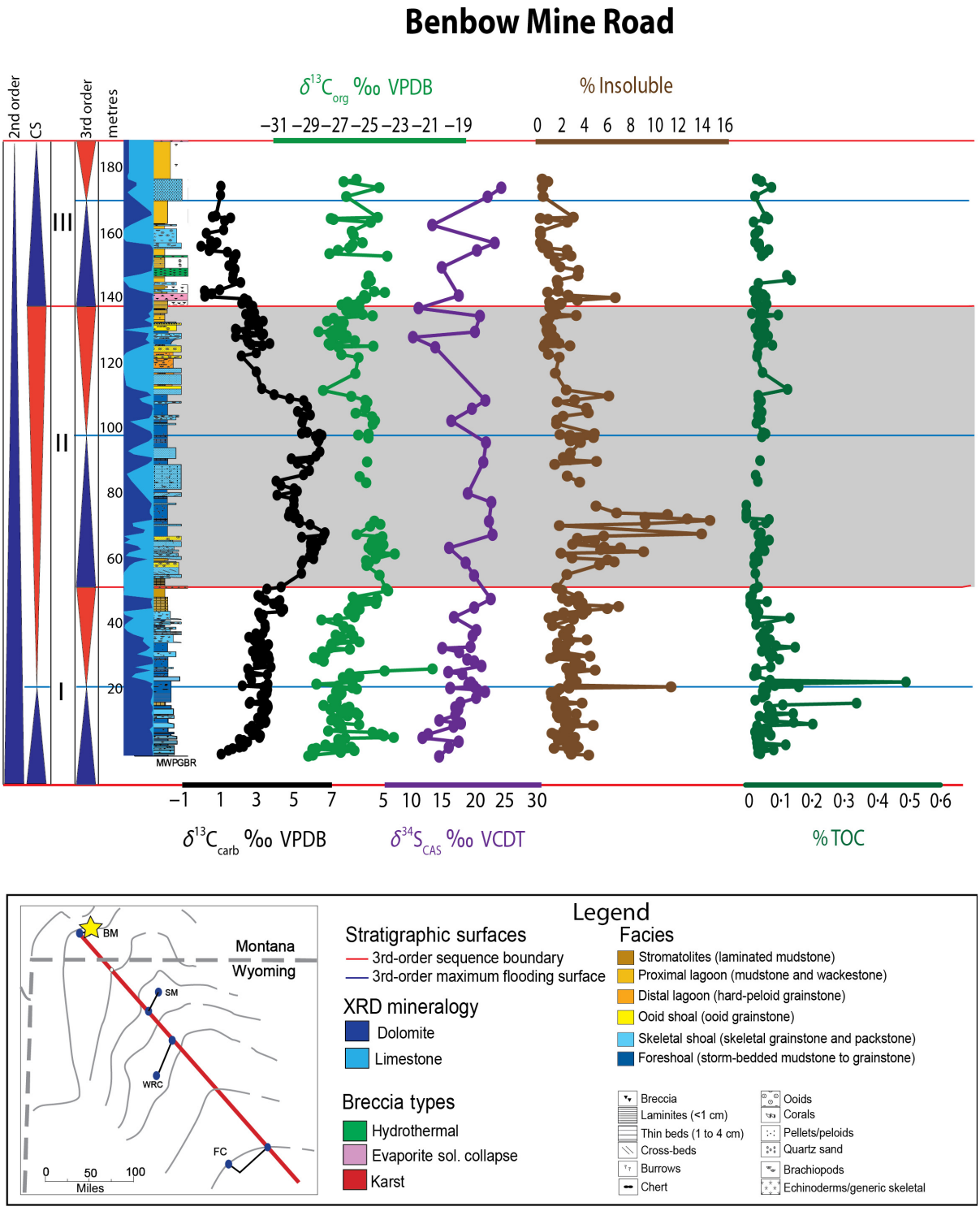

Fig. 6. Stratigraphic plots of geochemical records from Benbow Mine Road (BM; 45°22′25.3″N, 109°47′39.3″W), including carbonate mineralogy, carbonate $\delta^{13}C$ values (from Katz *et al.*, 2007), organic $\delta^{13}C$ values, $\delta^{34}S_{CAS}$ values, % acid insoluble material and % total organic carbon (TOC). Sequence stratigraphy and sedimentological descriptions from Smith *et al.* (2004). In the map of outcrop locations, the red line denotes the same transect as presented in Fig. 1 and the yellow star indicates the outcrop from which the data presented in this figure were collected. CS, Cycle Sets; FC, Freemont Canyon; SM, Sheep Mountain; VCDT, Vienna Canyon Diablo Troilite; VPDB, Vienna Pee Dee Belemnite; WRC, Wind River Canyon.

Importance of terrestrial input in the deposition of the Madison Limestone

In contrast to the change in bulk carbonate $\delta^{13}C$ values driven by global carbon cycling, the new dataset produced by this study emphasizes the importance of local depositional controls. Input of terrestrial materials to the marine environment during deposition of the Madison Limestone controlled several key features of the organic $\delta^{13}C$ values, TOC and acid-insoluble residue records. First, organic $\delta^{13}C$ values exhibit more variability than their counterpart bulk carbonate $\delta^{13}C$ values (Figs 3 to 6), which supports the interpretation of decoupled mechanisms driving the two records independently. If the variability in both the bulk carbonate and organic matter $\delta^{13}C$ values was driven by changes in the $\delta^{13}C$ value of the DIC, both records should reflect that change equally. Although the record from Sheep Mountain exhibits the clearest example of a positive change in $\delta^{13}C$ values of organic matter of all four outcrops measured, the peak $\delta^{13}C$ values of organic matter do not persist as long as the more positive bulk carbonate $\delta^{13}C$ values do (Figs 3 to 6).

In all sections, the positive excursion in $\delta^{13}C$ values of organic matter corresponds to the transgressive portion of Sequence II (Figs 3 to 6). Organic $\delta^{13}C$ values at Sheep Mountain change from −29 to −23‰ within the transgressive phase of the sequence, suggesting that the input of terrestrial organic matter might be playing a role in defining the organic $\delta^{13}C$ values of the bulk sedimentary organic matter. The $\delta^{13}C$ value of Early Mississippian terrestrial organic matter is thought to have increased from −25‰ to nearly −21‰ during this period, which has been interpreted to reflect changes in the atmospheric O_2/CO_2 ratio (Strauss & Peters-Kottig, 2003; Peters-Kottig *et al.*, 2006). In contrast to the isotopic compositions of marine and terrestrial organic matter in the recent geological record, Early Mississippian terrestrial organic matter was substantially more enriched in ^{13}C than its counterpart marine organic matter which averaged −28‰ during the same time period (Hayes *et al.*, 1999).

This observation is fundamental in understanding the possible impact that degradation of organic matter and recrystallization of the carbonate may have on the carbonate $\delta^{13}C$ record. Degradation of terrestrial organic matter in an

Table 1. Average values for carbonate $\delta^{13}C$ values [‰Vienna Pee Dee Belemnite (VPDB)], organic $\delta^{13}C$ values (‰ VPDB), $\delta^{34}S_{CAS}$ [‰Vienna Canyon Diablo Troilite (VCDT)], percent dolomite, percent total organic carbon (TOC), percent insoluble material and the concentration of carbonate associated sulphate (CAS; ppm) within the whole record, and then subdivided by sequence. Average values are listed with number of analyses in parentheses. NM, not measured.

	$\delta^{13}C_{carb}$	$\delta^{13}C_{org}$	$\delta^{34}S_{CAS}$	%Dol	%TOC	%Insol.	[CAS]
Whole record							
BM	+3·4 (193)	−26·1 (168)	+17·8 (56)	70 (187)	0·06 (174)	2·91 (189)	2800 (37)
SM	+3·6 (246)	−26·8 (224)	+17·8 (29)	57 (84)	NM	NM	1117 (25)
WRC	+2·5 (149)	−25·8 (78)	+14·8 (19)	97 (141)	0·04 (78)	1·36 (77)	292 (13)
FC	+0·7 (99)	−23·6 (97)	+13·9 (14)	81 (99)	0·04 (99)	2·84 (99)	NM
Sequence I							
BM	+3·1 (84)	−26·5 (82)	+17·4 (32)	78 (84)	0·07 (83)	2·74 (86)	3460 (16)
SM	+2·8 (65)	−27·6 (65)	+17·7 (6)	93 (20)	NM	NM	1160 (3)
WRC	+2·1 (32)	−26·3 (32)	+17·6 (6)	96 (32)	0·04 (32)	1·11 (32)	331 (5)
FC	+0·1 (29)	−24·6 (29)	+15·8 (4)	97 (29)	0·03 (29)	2·51 (29)	NM
Sequence II							
BM	+4·6 (78)	−25·7 (57)	+18·3 (17)	66 (70)	0·04 (62)	3·69 (71)	2236 (14)
SM	+4·9 (103)	−26·2 (103)	+19·0 (18)	45 (43)	NM	NM	1318 (17)
WRC	+3·9 (41)	−24·4 (41)	+11·5 (8)	96 (35)	0·06 (41)	1·63 (40)	224 (6)
FC	+2·3 (38)	−22·7 (37)	+13·5 (4)	93 (38)	0·05 (38)	3·25 (38)	NM
Sequence III							
BM	+1·2 (31)	−25·8 (29)	+18·9 (7)	61 (33)	0·05 (29)	1·65 (32)	2423 (7)
SM	+2·4 (78)	−26·8 (56)	+13·5 (5)	46 (21)	NM	NM	407 (5)
WRC	+1·9 (76)	−24·9 (5)	+16·8 (5)	97 (74)	0·03 (5)	0·76 (5)	398 (2)
FC	−0·6 (32)	−24·1 (31)	+13·0 (6)	52 (32)	0·03 (32)	2·66 (32)	NM

BM, Benbow Mine Road; FC, Freemont Canyon; SM, Sheep Mountain; WRC, Wind River Canyon.

Table 2. Correlation coefficients from linear regression analyses of the listed geochemical records. Values in parentheses are the number of analyses in the regression and the coefficients in bold type have P values <0·05. NM, not measured.

	BM	SM	WRC	FC
$\delta^{13}C_{carb}$ versus $\delta^{13}C_{org}$	**0·11** (162)	**0·25** (224)	**0·11** (78)	**0·13** (97)
$\delta^{13}C_{carb}$ versus $\delta^{34}S_{CAS}$	0·04 (55)	**0·49** (27)	**0·44** (18)	0·04 (13)
$\delta^{13}C_{org}$ versus $\delta^{34}S_{CAS}$	0·03 (55)	**0·25** (26)	**0·29** (13)	**0·30** (13)
TOC versus $\delta^{34}S_{CAS}$	0·00 (55)	NM	0·00 (14)	0·00 (13)
%Insol versus $\delta^{34}S_{CAS}$	0·04 (55)	NM	0·05 (14)	0·13 (13)
[CAS] versus $\delta^{34}S_{CAS}$	0·04 (37)	**0·25 (25)**	0·06 (12)	NM

BM, Benbow Mine Road; FC, Freemont Canyon; SM, Sheep Mountain; WRC, Wind River Canyon.

oxic ocean during the Early Mississippian would result in a source of relatively ^{13}C-enriched CO_2 to the DIC pool compared to the degradation of contemporaneous marine organic matter. However, terrestrial organic matter has been shown to be more resistant to degradation than its counterpart marine organic material (Freudenthal *et al.*, 2001; Lehmann *et al.*, 2002; Lamb *et al.*, 2006; Huguet *et al.*, 2008) and therefore was less likely to contribute to the DIC pool during deposition of the Madison Limestone. As a result, changes in the DIC pool were more likely to be driven by enhanced drawdown of CO_2 in the terrestrial realm. Finally, in contrast to the model of Oehlert & Swart (2014) where subaerial exposures drive the oxidation and recrystallization reactions causing coupled $\delta^{13}C$ excursions in recent carbonates and organic matter, the excursions in the Madison Limestone are associated with the transgression and maximum flooding surface of Sequence II. In concert, these observations support the interpretation that the transport of terrestrial organic materials probably impacted the $\delta^{13}C$ values of the sedimentary organic matter, without significantly impacting the $\delta^{13}C$ values of syndepositional marine carbonates.

Further support comes from the trend in more positive organic $\delta^{13}C$ values during the regressive portion of Sequence II at Sheep Mountain compared to those at the more proximal sites. While organic $\delta^{13}C$ values from Freemont Canyon and Wind River Canyon remain positive during the regression, at Sheep Mountain they decrease towards more marine organic $\delta^{13}C$ values below the maximum flooding surface. Records from Benbow Mine Road do not show a significant positive excursion in organic $\delta^{13}C$ values during this sequence. This observation suggests that increasing distance from the terrestrial source of organic material with a higher organic $\delta^{13}C$ value dampens the extent and duration of the changes observed associated with Sequence II. This scenario is consistent with a mixing model between terrestrial and marine organic material driven by sea-level oscillations, similar to that observed on the Great Bahama Bank, where Oehlert *et al.* (2012) found that isotopic differences in the sources of organic carbon could produce an excursion in organic $\delta^{13}C$ values related to sea-level driven source change. Mixing between different organic matter sources has also been suggested as a mechanism during the Ediacaran (Lee *et al.*, 2013), demonstrating that syndepositional mixing of isotopically distinct end-members is not necessarily constrained to modern environments.

Similar to the organic $\delta^{13}C$ values, the IR also did not exhibit one consistent change towards higher values at all locations (Figs 3 to 6). In fact, the percent IR actually displays multiple pulses of terrestrially derived insoluble materials within the transgressive phase of the sequence which is in concert with the cyclic nature of the facies within the sequence. In particular, the most proximal location, Freemont Canyon, exhibits three pulses of terrestrial inputs of IR within Sequence II (Fig. 3). Furthermore, the highest proportion of IR preserved in the sediments was observed at this location and decreases slightly with distance from the Transcontinental Arch (Figs 3 to 6), suggesting that the locations closest to the Transcontinental Arch may have experienced the most significant fertilization impacts from the weathered nutrients transported from the terrestrial to marine realm.

The higher percentage of TOC in the proximal settings also supports the interpretation that increased productivity was the likely causative factor for persistently positive organic $\delta^{13}C$ values in the regressive phase of Sequence II. At both Wind River Canyon and Freemont Canyon,

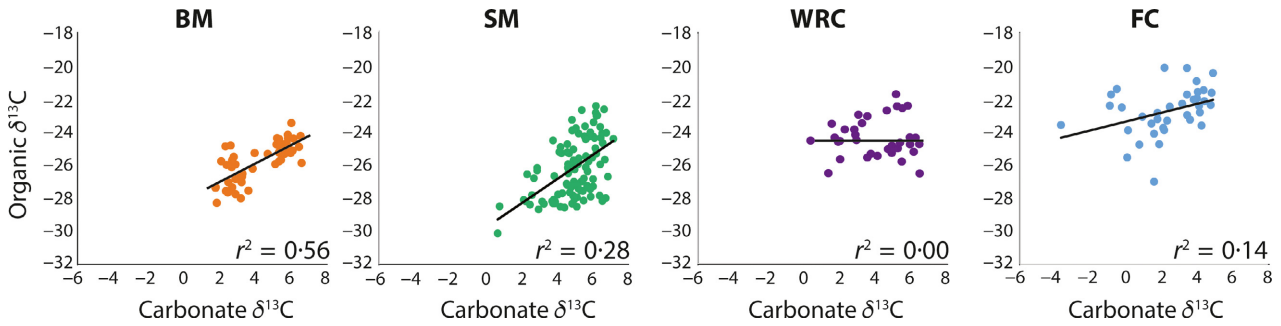

Fig. 7. Correlations between Sequence II carbonate and organic δ^{13}C values from each outcrop along the proximal to distal transect (BM, Benbow Mine Road; FC, Freemont Canyon; SM, Sheep Mountain; WRC, Wind River Canyon).

the TOC values are highest in the regressive phase of Sequence II (Figs 3 to 6), where it is likely that the runoff of weathered materials from the Transcontinental Arch relieved a nutrient limitation and enhanced the productivity rates. At both locations, TOC values start to decrease towards the sequence boundary between Sequences II and III, suggesting that the enhanced rates of marine productivity were declining towards the end of Sequence II. This pattern probably explains why organic δ^{13}C values begin to fall back towards pre-excursion values just prior to the sequence boundary.

Geochemical constraints on the initiation of excursion in carbonate δ^{13}C values

The role of land plants

Whilst various biogeochemical and tectonic forcing mechanisms have been proposed to explain the initiation of the largest positive excursion in bulk carbonate δ^{13}C values in the Phanerozoic, the results of this study suggest that the rise of vascular plants may have played the most significant role in generating the change. A review of Palaeozoic tropical rainforests suggests that the efficient photosynthetic mechanism of plants at this time could have resulted in an extremely fast growth rate (Cleal & Thomas, 2005), and such an increase in the burial of terrestrial plant vascular tissue in peat bogs in the Palaeozoic (Berner, 1994, 1998; Berner & Kothvala, 2001) would have significantly perturbed the global carbon cycle.

The evolution of vascular plants in the terrestrial realm occurred in the Devonian as observed by palaeobotanical data (Algeo *et al.*, 1995), and is evidenced by a distinct drop in atmospheric levels of CO_2 in both modelling and geochemical studies (Berner, 1994, 1998; Berner & Kothvala, 2001). Long-term carbon sequestration by such coal forests has been estimated to be between 108 t ha^{-1} per annum and 390 t ha^{-1} per annum, resulting from higher Palaeozoic growth rates when compared to modern tropical rainforests (Cleal & Thomas, 2005). This intense drawdown of CO_2 during the Devonian would have set up a much smaller atmospheric reservoir of CO_2, making the reduced size of the atmospheric reservoir of CO_2 during the Carboniferous particularly sensitive to changes in the rate and location of organic carbon burial. The more cosmopolitan distribution of land plants in the Carboniferous resulted in extensive deposition of lignin-rich organic material in bogs around the world (Berner & Kothvala, 2001), resulting in an even further drawdown of CO_2 during this time. In addition, exudation of organic acids by roots and the metabolic recycling of respired carbon acted to enhance phosphate weathering on land, which acted to increase aquatic primary production (Igamberdiev & Lea, 2006). As a result, the evolution of terrestrial plants during the Devonian impacted rates of organic carbon burial on both land and in the oceans.

The significant drawdown of CO_2 by vascular land plants would have increased the O_2/CO_2 ratio in the atmosphere, which has been shown to impact plant metabolism and change the fractionation between plant tissue produced via photosynthesis and atmospheric CO_2 (Farquhar *et al.*, 1982; Strauss & Peters-Kottig, 2003). The change in the O_2/CO_2 ratio has been discussed as a possible proxy for atmospheric composition over geological time (Beerling & Berner, 2000; Berner *et al.*, 2000; Beerling *et al.*, 2002). Such metabolic changes and subsequent shifts towards more positive organic δ^{13}C values in terrestrial plants during this time period would have imparted more positive δ^{13}C values on both

the atmosphere and DIC in the surface waters of the ocean. Therefore, the global shift towards more positive $\delta^{13}C$ values recorded in the Madison Limestone and its age equivalents was a function of two compounding factors: (i) the enhanced burial of organic matter in the terrestrial realm would have shifted the $\delta^{13}C$ value of the atmosphere towards more positive values; and (ii) the change in the $\delta^{13}C$ value of the terrestrial organic matter itself towards more positive values would have acted to further enhance the positive shift in the $\delta^{13}C$ values of the marine carbonates precipitated in equilibrium with the DIC pool during this perturbation.

Therefore, this multi-proxy evaluation of the largest Phanerozoic positive excursion in bulk carbonate $\delta^{13}C$ values provides support for the interpretation that the large positive shift in carbonate $\delta^{13}C$ values in the Early Mississippian reflected a perturbation to the global carbon cycle, rather than a local or diagenetic effect. As previously described, the change in bulk carbonate $\delta^{13}C$ values occurs simultaneously worldwide; in each of the outcrops in the western US (Mii *et al.*, 1999; Gill *et al.*, 2007; Katz *et al.*, 2007; Koch *et al.*, 2014) to the Dinant Basin (Belgium; Saltzman *et al.*, 2004) and the Ural Mountains (Saltzman *et al.*, 2004). This worldwide perturbation requires a global driver that probably affected the atmospheric reservoir of CO_2. In addition to the carbonate record of bulk $\delta^{13}C$ values, trends in organic $\delta^{13}C$ values at each of the study locations supports the introduction of terrestrial organic carbon to the marine realm with the onset of the transgression, peaking in most locations at the maximum flooding surface of Sequence II (Figs 3 to 6). Part of this increase is attributable to mixing between terrestrial and marine organic matter through time, accompanied by an increase in the isotopic composition of the DIC.

Source mixing, or in this case, increased contributions of terrestrial organic carbon, is postulated to influence the organic $\delta^{13}C$ values. The isotopic difference between marine and terrestrial organic matter (Hayes *et al.*, 1999; Strauss & Peters-Kottig, 2003) sets up a two end-member mixing, where increases in the bulk organic matter $\delta^{13}C$ values may be caused by increased contributions of terrestrially derived organic matter. Such syndepositional, two end-member mixing, has been observed in Pleistocene records of bulk carbonate and organic $\delta^{13}C$ values from the slope of the Great Bahama Bank, where sea-level oscillations controlled the contributions of isotopically positive, platform-derived carbonate and organic matter with pelagic carbonates and organic carbon with comparatively more negative $\delta^{13}C$ values (Oehlert *et al.*, 2012). Furthermore, the average $\delta^{13}C$ values of the sedimentary organic matter become increasingly more positive proximal to the transcontinental arch for Sequence II, suggesting that terrestrial organic carbon is present in higher abundances in Freemont Canyon (−23·6‰; Fig. 2) than in Benbow Mine Road (−26·1‰; Fig. 6). In addition to the organic $\delta^{13}C$ values, the spread of vascular land plants is also supported by the trends in the insoluble materials in the transect of outcrops, likely to result from enhanced weathering by land plants (Igamberdiev & Lea, 2006). Peaks in insoluble materials were observed to be associated with the maximum flooding surface at each of the outcrops and the highest average concentration of insoluble materials was consistently observed within Sequence II (Table 1; Figs 3 to 6). These increases in the concentration of insoluble materials occur concurrently with the increase in the organic $\delta^{13}C$ values, which is thought to be related to the introduction of terrestrial organic matter. The simultaneous deposition of increased terrestrial–insoluble materials and organic carbon linked by the maximum flooding surface supports the colonization of the Transcontinental Arch by terrestrial plants which enhanced weathering on land.

No geochemical evidence for anoxia during deposition of the Madison Limestone

A correlation between $\delta^{34}S_{CAS}$ and bulk carbonate $\delta^{13}C$ values has been interpreted as evidence of anoxia (Jenkyns, 2010). However, in the Madison sections, the $\delta^{34}S_{CAS}$ values exhibit very different behaviours at each location, suggesting that in some of the locations local environmental factors may have been important in governing the $\delta^{34}S_{CAS}$ values. Diagenetic alteration has been shown to alter the concentration of CAS, while maintaining the original $\delta^{34}S_{CAS}$ values (Gill *et al.*, 2011; Fichtner *et al.*, 2017), and therefore, the $\delta^{34}S_{CAS}$ records are interpreted to reflect changes in the contemporaneous sulphur cycle. The $\delta^{34}S_{CAS}$ values from the most proximal location, Freemont Canyon (Fig. 3), exhibit a negative excursion at the maximum flooding surface, suggesting that freshwater run off and weathered materials from the Transcontinental Arch probably caused the seawater $\delta^{34}S_{CAS}$ signature to be overwhelmed by the $\delta^{34}S_{CAS}$ value of weathered terrestrial sulphide minerals or even degrading coals. Previous work shows that the average $\delta^{34}S$

composition of average sedimentary sulphides for the Palaeozoic exhibits a trend from 0‰ around 500 Ma, to nearly −30‰ (V-CDT) at the Permo–Triassic Boundary 252 Ma (Canfield & Kump, 2013). In addition, organic sulphur during this time was depleted in ^{34}S relative to contemporaneous seawater values (Canfield & Kump, 2013), suggesting that weathering of sulphide minerals or from weathering of organic matter during the deposition of the Madison Limestone could have contributed to the negative shifts in $\delta^{34}S_{CAS}$ observed at Wind River Canyon and Freemont Canyon in the transgressive portion of Sequence II (Figs 3 and 4).

The $\delta^{34}S_{CAS}$ values in the regressive phase of Sequence II at Freemont Canyon and Wind River Canyon exhibit different behaviours. The $\delta^{34}S_{CAS}$ values from Freemont Canyon spike to more positive values in this regressive phase, while $\delta^{34}S_{CAS}$ values from Wind River Canyon remain persistently low. The differences in behaviour between the two proximal sites could be attributed to small sulphate reservoirs, or to weathering of older continental evaporites which contribute only to the $\delta^{34}S$ values at Freemont Canyon as a result of proximity. From a mass-balance perspective, locally small sulphate reservoirs would be more sensitive to changes in the rate or isotopic composition of different fluxes into the shallow marine environment, thus producing more variable $\delta^{34}S_{CAS}$ values. In contrast to previous work which suggested that the size of the sulphate reservoir increased prior to deposition of the Madison Limestone (Gill *et al.*, 2007), these results suggest that, at least in the case of the proximal ramp setting, the sulphate reservoir may have been small and thus susceptible to change via weathering input.

Evaporite deposits have been documented from the Middle Ordovician through to the Tournaisian in regions around the Transcontinental Arch and the Williston Basin, and describe depositional environments ranging from sabkha-type environments to evaporite–solution breccias (Johnson, 1992). Mapping of evaporitic facies in the time-equivalent Ballagan Formation in Nova Scotia and Scotland shows the presence of gypsum nodules in siltstone, dolostone with gypsum and halite in seven of the eight studied sections in depositional environments described as coastal tropical wetlands (Millward *et al.*, 2018). The observation of evaporites around the globe during this period demonstrates that evaporite deposition during this period was not a locally restricted phenomenon, and is likely to reflect conducive palaeoclimatic conditions (Millward *et al.*, 2018).

In contrast to proximal locations, Sheep Mountain and Benbow Mine Road exhibit positive changes in $\delta^{34}S_{CAS}$ values within Sequence II (Figs 5 and 6). This is interpreted to reflect a more open and larger sulphate reservoir when compared to the more restricted environments at Freemont Canyon and Wind River Canyon. Positive excursions in $\delta^{34}S_{CAS}$ values that co-occur with positive changes in carbonate $\delta^{13}C$ values have been interpreted to result from periods of water-column anoxia (Jenkyns, 2010). However, the correlation coefficients between bulk carbonate $\delta^{13}C$ and $\delta^{34}S_{CAS}$ values from this study are not consistent with the interpretation of a period of anoxia. The strongest positive correlation occurs at Sheep Mountain ($r^2 = 0{\cdot}59$, $P < 0{\cdot}05$, $n = 27$), while there is no statistical correlation between bulk carbonate $\delta^{13}C$ and $\delta^{34}S_{CAS}$ values at Benbow Mine Road ($r^2 = 0{\cdot}23$, $P > 0{\cdot}05$, $n = 55$). The lack of a statistically significant positive correlation this site suggests that these two locations are not recording a period of anoxia, since both locations are not recording the classic coupled response of the bulk carbonate $\delta^{13}C$ and $\delta^{34}S_{CAS}$ values (Jenkyns, 2010). Similar to previously measured $\delta^{34}S_{CAS}$ values from a section, including the excursion in bulk carbonate $\delta^{13}C$ values at the Kinderhookian–Osagean (Gill *et al.*, 2007), the $\delta^{34}S_{CAS}$ values from Benbow Mine Road are relatively invariant. Furthermore, sedimentological evidence of anoxia, including the deposition and preservation of black organic-rich mudrock has not been observed in these outcrops (Katz *et al.*, 2007; Buoniconti, 2008; Katz, 2008). Since recent studies have shown that the $\delta^{34}S_{CAS}$ values of both recent (Gill *et al.*, 2008) and Triassic carbonates (Fichtner *et al.*, 2017) are maintained during diagenesis, other controls on variability in the $\delta^{34}S_{CAS}$ values, such as freshwater runoff and contributions of sulphate from terrestrial evaporites, are considered as possible mechanisms driving the variability in $\delta^{34}S_{CAS}$ values observed in the Madison Limestone outcrops presented in this study.

The observation that carbonate $\delta^{13}C$ and $\delta^{34}S_{CAS}$ values are positively correlated at Sheep Mountain and decoupled at Benbow Mine Road requires additional consideration. Previous workers have pointed out that carbon and sulphur have different residence times in the ocean (Kampschulte *et al.*, 2001; Jones & Fike, 2013, Turchyn & Schrag, 2004), with carbon having a two-order of magnitude smaller residence time in

the oceans than sulphur (Walker, 1986). As a result, perturbations in the carbon cycle may occur without coupled $\delta^{34}S$ responses (Kump & Garrels, 1986) or with a temporal lag (Jones & Fike, 2013) leading to a lack of statistically significant correlation between coeval carbonate $\delta^{13}C$ and $\delta^{34}S_{CAS}$ records. Analysis of the sedimentary pyrite $\delta^{34}S$ records could provide important insight into the mechanisms controlling the lack of correlation between carbonate $\delta^{13}C$ and $\delta^{34}S_{CAS}$ records observed at Benbow Mine Road, contrasted with the high degree of correlation documented in samples from Sheep Mountain. Another possible explanation includes the progressive decoupling of the carbon–sulphur system throughout the Palaeozoic resulting from increasing concentrations of seawater sulphate, which make the oceans less sensitive to changes in flux (Gill *et al.*, 2007). An alterative explanation could also be that substantial organic carbon burial in the terrestrial realm perturbed the carbon cycle, but a lack of coupled pyrite burial prevented such a perturbation from affecting the sulphur cycle (Gill *et al.*, 2007). This observation is consistent with the conclusions herein, which suggest that the perturbation driving the positive shift in carbonate $\delta^{13}C$ values during Sequence II is driven by enhanced organic carbon burial on land.

The role of sea-level transgression

Another proposed mechanism for the change in bulk carbonate $\delta^{13}C$ values is the large marine transgression (Sonnenfeld, 1996; Smith *et al.*, 2004) observed in Sequence II and the associated increase in productivity (Katz *et al.*, 2007). However, although the sea-level transgression observed in Sequence II had significant impacts on the sedimentology, stratigraphy and transport of terrestrial-derived materials (Katz *et al.*, 2007), the results of this study suggest that a transgression alone could not have initiated the large positive shift in bulk carbonate $\delta^{13}C$ values. Furthermore, within the context of geological time, sea-level transgressions are relatively common, while changes in the bulk carbonate $\delta^{13}C$ values of this magnitude do not occur frequently.

The organic $\delta^{13}C$ values from each of the four locations demonstrate changes towards more positive values during the transgressive phase of Sequence II, a change interpreted to reflect increasing contributions of terrestrial organic material with more positive organic $\delta^{13}C$ values (Figs 3 to 6). Peaks in insoluble materials are also observed at the maximum flooding surface associated with Sequence II at Freemont Canyon and Wind River Canyon (Figs 3 and 4), as well as an increase in the abundance of argillaceous materials in the Sheep Mountain Anticline (Fig. 4; Sonnenfeld, 1996). It is therefore possible that the introduction of insoluble materials during this transgression increased nutrient availability and provided for enhanced marine productivity during the regression. The trend of persistently positive organic $\delta^{13}C$ values observed in the Sequence II regressive phase suggests that a period of increased productivity may have contributed to the sustained positive organic $\delta^{13}C$ values (Figs 3 to 6). Evidence for enhanced productivity may also be seen in the increased average TOC compositions observed in the regressive portion of Sequence II compared to the transgressive portions of Sequence II.

Decoupled mechanisms for the changes in carbonate and organic $\delta^{13}C$ values

One of the most interesting results in this study is the correlation between the bulk carbonate $\delta^{13}C$ values published by Katz *et al.* (2007) and the organic $\delta^{13}C$ values in this paper (Fig. 7). Statistically significant correlations are observed at each outcrop, although with relatively low r^2 values, which range from 0·11, ($P < 0·05$) at both the middle ramp setting (Wind River Canyon, $n = 97$) and the 0·13 at the most distal setting (Benbow Mine Road, $n = 162$), ($P < 0·05$) at the most proximal setting (Freemont Canyon, $n = 97$). The highest observed correlation between bulk carbonate and organic $\delta^{13}C$ values is observed at Sheep Mountain ($r^2 = 0·25$, $P < 0·05$, $n = 224$). Many studies would interpret a significant correlation as evidence that the change in bulk carbonate $\delta^{13}C$ values was definitively the result of a perturbation to the global carbon cycle. However, this requires the assumption that an equal shift in the bulk carbonate and organic $\delta^{13}C$ values is observed, and that these paired shifts were the result of a change in the $\delta^{13}C$ composition of the DIC.

In the case of the Madison Limestone, the relatively low r^2 values and the nature of the stratigraphic relationship between the bulk carbonate and organic $\delta^{13}C$ values suggests that it is unlikely that the mechanism that caused the positive changes in the bulk carbonate $\delta^{13}C$ values was also the primary driver for the changes in organic $\delta^{13}C$ values. A more likely explanation is that the bulk carbonate and organic $\delta^{13}C$ values are controlled by separate factors that fortuitously generated positive excursions at the

same time within Sequence II. The bulk carbonate $\delta^{13}C$ values are interpreted to be controlled by a large change in the $\delta^{13}C$ value of the contemporaneous marine DIC resulting from a perturbation to the global carbon cycle driven by the evolution and proliferation of vascular land plants and increased organic matter (OM) burial in wetlands.

In contrast, the organic $\delta^{13}C$ values are interpreted to be controlled primarily by changes in the proportion of organic matter derived from the terrestrial realm during the transgressive portion of Sequence II. Records of the percent insoluble material preserved in the samples provide support for this interpretation (Figs 3 to 6). Peaks in the insoluble material are observed in the transgressive phase of Sequence II, suggesting that large amounts of weathered materials were transported from the Transcontinental Arch to the adjacent shallow carbonate ramp. During the regressive phase of the sequence, these additional weathered materials probably acted to relieve a nutrient limitation, increasing marine organic matter productivity in the nearshore waters. This interpretation is further supported by the record of organic $\delta^{13}C$ values from these outcrops (Figs 3 to 6).

The transgressive portion of Sequence II is associated with an increase in the organic $\delta^{13}C$ values that peaks at the maximum flooding surface at each location, followed by sustained positive organic $\delta^{13}C$ values that persist even while bulk carbonate $\delta^{13}C$ values fall back towards pre-excursion values. The initial increase in organic $\delta^{13}C$ values during the transgressive phase is interpreted to reflect an increasing proportion of terrestrial organic carbon that was mobilized by ravinement erosion and released into the marine realm. In contrast to the Cenozoic and Mesozoic, when marine organic matter typically contains more ^{13}C than contemporaneous marine organic matter, trends in the isotopic composition of Mississippian are the inverse, where terrestrial organic carbon (-21 to $-23‰$) is enriched in ^{13}C relative to the marine organic matter (-26 to $-28‰$; Hayes *et al.*, 1999; Peters-Kottig *et al.*, 2006). Therefore, as the transgression progressed to the maximum flooding surface, the proportion of terrestrial organic carbon would reach a peak. Similar what has been observed in the modern Great Bahama Bank, mixing of two isotopically distinct sources of organic carbon can produce changes in the organic $\delta^{13}C$ values of sedimentary organic matter that is related to sea-level oscillations and not to a perturbation to the global carbon cycle (Oehlert *et al.*, 2012).

The persistent positive organic $\delta^{13}C$ values in the regressive phase of Sequence II are attributed to the enhanced rates of productivity caused by the input of terrestrially derived nutrients. Furthermore, terrestrial organic matter is more resistant to degradation reactions (Hatch & Leventhal, 1997; Prahl *et al.*, 1997; Freudenthal *et al.*, 2001), causing the preferential preservation of sedimentary organic matter with more positive $\delta^{13}C$ values during this time period compared to sections with a higher proportion of marine organic matter. These weathered materials, introduced during the time of maximum flooding, essentially fertilized the productivity of this shallow marine ramp, resulting in increased rates of organic carbon production that reduced the fractionation between DIC and organic carbon. It is unlikely that these persistently high organic $\delta^{13}C$ values are caused by contributions of terrestrial organic carbon during the regressive phase, because the proportions of insoluble materials are much lower, suggesting that terrestrial material, either terrestrial organic matter or weathered nutrients, did not reach the middle ramp during the regressive phase of Sequence II.

While bulk carbonate and organic $\delta^{13}C$ values change towards more positive values in the transgressive portion of Sequence II, the records and the mechanisms that drive their $\delta^{13}C$ values become decoupled during the regressive phase. This observation demonstrates the lack of a unified driving mechanism, such as changes in global carbon cycling as the cause of the positive change. When bulk carbonate $\delta^{13}C$ values begin to decrease towards pre-excursion values immediately after the maximum flooding surface, the organic $\delta^{13}C$ values remain persistently positive compared to early values (Figs 3 to 6). While the perturbation to the global carbon cycle dramatically changed the $\delta^{13}C$ value of the marine DIC, this decoupling of the carbonate and organic $\delta^{13}C$ values suggests that other factors played a more significant role in generating the $\delta^{13}C$ value of the marine organic matter. This is a rather surprising finding because it means that a perturbation to the global carbon cycle that was substantial enough to produce one of the largest positive excursions in Phanerozoic bulk carbonate $\delta^{13}C$ values did not exert an overriding control on the $\delta^{13}C$ values of the co-occurring sedimentary organic matter.

Implications for chemostratigraphy

The observation that one of the largest perturbations to the Phanerozoic carbon cycle was not capable of generating strongly correlated records of carbonate and organic $\delta^{13}C$ values is an important new consideration for interpretations of such covariance. In concert with other published studies investigating the significance of covariance in both modern and ancient depositional environments, the results of this study highlight the importance of a thorough characterization of the sediment and organic matter sources, sedimentation pathways, sequence stratigraphy and sea-level history, diagenetic history, evolutionary events, the possibility of both syndepositional and post-depositional mixing, organic matter recycling and spatial geochemical gradients when making accurate interpretations of the significance of shifts in carbonate $\delta^{13}C$ values and creating chemostratigraphic correlations (Johnston *et al.*, 2012; Oehlert *et al.*, 2012; Lee *et al.*, 2013; Oehlert & Swart, 2014; Wang *et al.*, 2016; Swart & Oehlert, 2018).

CONCLUSIONS

The amplitude of the excursion in Lower Mississippian bulk carbonate $\delta^{13}C$ values observed in the Madison Limestone suggests a change in the global carbon cycle that requires a unique set of environmental conditions and initiation mechanisms, so that such a large change in bulk carbonate $\delta^{13}C$ values is not observed in the Phanerozoic after this time period. The fact that the positive excursion in bulk carbonate $\delta^{13}C$ values is observed in marine carbonates both regionally (Saltzman, 2002; Gill *et al.*, 2011; Koch *et al.*, 2014) and around the world (Berner & Raiswell, 1983; Berner, 1990; Berner & Petsch, 1998; Saltzman, 2002; Saltzman *et al.*, 2004) is consistent with the interpretation that points to a perturbation to the global carbon cycle, rather than local or post-depositional processes. In this case, the evolution of vascular land plants is interpreted to be the driver for one of the largest Phanerozoic positive excursions in carbonate $\delta^{13}C$ values.

Furthermore, these results suggest that the evolution of this new terrestrial sink in the global carbon budget and its impact on the global carbon cycle might have been locally amplified within the Madison Limestone by a global sea-level rise (Katz *et al.*, 2007), as well as the introduction of weathering products to relieve nutrient limitation by the local tectonic uplift of the Antler Foreland (Saltzman *et al.*, 2000). In contrast, persistently positive organic $\delta^{13}C$ values coupled with increased concentrations of acid-insoluble material in the regressive section of Sequence II support the interpretation that the introduction of terrestrial materials played an important role in generating the geochemical records observed in Madison Limestone.

The proliferation of vascular plants in the Carboniferous not only destabilized the global carbon cycle, but also played an important role in the weathering of terrestrial materials, and contributed isotopically distinct organic matter to the marine environment. When mixed with marine organic matter, terrestrial organic material provides a ^{13}C enriched end-member and creates a two end-member mixing system in the Lower Mississippian. Although the mechanisms that drove the transition towards more positive organic and bulk carbonate $\delta^{13}C$ values are related to the evolution of vascular land plants, the two records remain unpaired through one of the largest excursions in carbonate $\delta^{13}C$ values in the Phanerozoic. These results lead to a significant theoretical debate: if this unique evolutionary perturbation could not generate coupled responses in the carbonate and organic $\delta^{13}C$ values, what type of event would?

ACKNOWLEDGEMENTS

This work was supported by the NSF grant OCE 0825577 to PKS and the Industrial Associates of the CSL – Center for Carbonate Research at the University of Miami (UM). The authors declare no conflict of interest, and would like to acknowledge helpful conversations with Benjamin Gill, Matthew Saltzmann, Taury Smith and Matthew Buoniconti. The authors would like to acknowledge the insightful comments of two anonymous reviewers which improved this manuscript.

REFERENCES

Ader, M., **Macouin, M.**, **Trindade, R.I.F.**, **Hadrien, M.H.**, **Yang, Z.**, **Sun, Z.** and **Besse, J.** (2009) A multilayered water column in the Ediacaran Yangtze platform? Insights from carbonate and organic matter paired $\delta^{13}C$. *Earth Planet. Sci. Lett.*, **288**, 213–227.

Algeo, T.J., **Berner, R.A.**, **Maynard, J.B.** and **Scheckler, S.E.** (1995) Late Devonian oceanic anoxic events and biotic crises: "Rooted" in the evolution of vascular land plants? *GSA Today*, **5**, 64–66.

Beerling, D.J. and **Berner, R.A.** (2000) Impact of a Permo-Carboniferous high O_2 event on the terrestrial carbon cycle. *Proc. Natl Acad. Sci.*, **97**, 12428–12432.

Beerling, D.J., **Lake, J.A.**, **Berner, R.A.**, **Hickey, L.J.**, **Taylor, D.W.** and **Royer, D.L.** (2002) Carbon isotope evidence implying high O_2/CO_2 ratios in the Permo-Carboniferous atmosphere. *Geochim. Cosmochim. Acta*, **66**, 3757–3767.

Berner, R.A. (1990) Atmospheric carbon dioxide levels over phanerozoic time. *Science*, **249**, 1382–1386.

Berner, R.A. (1994) GEOCARB II: A revised model of Atmospheric CO_2 over Phanerozoic time. *Am. J. Sci.*, **291**, 56–61.

Berner, R.A. (1998) The carbon cycle and carbon dioxide over Phanerozoic time: the role of land plants. *Phil. Trans. Roy. Soc. B Biol. Sci.*, **353**, 75–82.

Berner, R.A. (2002) Examination of the hypotheses for the Permo-Triassic boundary extinction by carbon cycle modeling. *Proc. Natl Acad. Sci. USA*, **99**, 4172–4177.

Berner, R.A. and **Kothvala, Z.** (2001) GEOCARB III: A revised model of Atmospheric CO_2 over Phanerozoic time. *Am. J. Sci.*, **301**, 182–204.

Berner, R.A. and **Petsch, S.** (1998) The sulfur cycle and atmospheric oxygen. *Science*, **282**, 1426–1427.

Berner, R.A. and **Raiswell, R.** (1983) Burial of organic carbon and pyrite sulphur in sediments over Phanerozoic time: A new theory. *Geochim. Cosmochim. Acta*, **47**, 855–862.

Berner, R.A., **Petsch, S.T.**, **Lake, J.A.**, **Beerling, D.J.**, **Popp, B.N.**, **Lane, R.S.**, **Laws, E.A.**, **Westley, M.B.**, **Cassar, N.**, **Woodward, F.I.** and **Quick, W.P.** (2000) Isotope fractionation and atmospheric oxygen: implications for Phanerozoic O_2 Evolution. *Science*, **287**, 1630–1633.

Bruckschen, P., **Oesmann, S.** and **Veizer, J.** (1999) Isotope stratigraphy of the European Carboniferous: proxy signals for ocean chemistry, climate and tectonics. *Chem. Geol.*, **161**, 127–163.

Buoniconti, M.R. (2008) The evolution of the carbonate shelf margins and fill of the Antler Foreland Basin by prograding Mississippian carbonates, Northern US Rockies. PhD Dissertation, University of Miami, Coral Gables, FL, 436 pp.

Canfield, D.E. and **Kump, L.R.** (2013) Carbon cycle makeover. *Science*, **6119**, 533–534.

Caravaca, G., **Thomazo, C.**, **Vennin, E.**, **Olivier, N.**, **Coquerez, T.**, **Escarguel, G.**, **Fara, E.**, **Jenks, J.F.**, **Bylund, K.G.**, **Stephen, D.A.** and **Brayard, A.** (2017) Early Triassic fluctuations in the global carbon cycle: New evidence from paired carbon isotopes in the western USA basin. *Global Planet. Change*, **154**, 10–22.

Cleal, C.J. and **Thomas, B.A.** (2005) Palaeozoic tropical rainforests and their effect on global climates: is the past the key to the present? *Geobiology*, **3**, 13–31.

Coplen, T.B., **Brand, W.A.**, **Gehre, M.**, **Gröning, M.**, **Meijer, H.A.J.**, **Toman, B.** and **Verkouteren, M.** (2006) New guidelines for $\delta^{13}C$ measurements. *Anal. Chem.*, **78**, 2439–2441.

Cramer, B.D. and **Saltzman, M.R.** (2007) Early Silurian paired $\delta^{13}C_{carb}$ and $\delta^{13}C_{org}$ analyses from the Midcontinent of North America: Implications for paleoceanography and paleoclimate. *Palaeogeogr. Palaeoclimatol. Palaeoecol.*, **256**, 195–203.

Crowell, J. (1999) Pre-Mesozoic ice ages: Their bearing on understanding the climate system. *EOS Trans. Am. Geophys. Union*, **81**, 1–570.

Elrick, M. and **Read, J.** (1991) Cyclic ramp-to-basin carbonate deposits, Lower Mississippian, Wyoming and Montana: a combined field and computer modeling study. *J. Sediment. Res.*, **61**, 1194–1224.

Farquhar, G.D., **O'Leary, M.H.** and **Berry, J.A.** (1982) On the relationship between carbon isotope discrimination and the intercellular carbon dioxide concentration in leaves. *Aust. J. Plant Physiol.*, **9**, 121–137.

Fichtner, V., **Strauss, H.**, **Immenhauser, A.**, **Buhl, D.**, **Neuser, R.D.** and **Niedermayr, A.** (2017) Diagenesis of carbonate associated sulfate. *Chem. Geol.*, **463**, 61–75.

Freudenthal, T., **Wagner, T.**, **Wenzhoffer, F.**, **Zabel, M.** and **Wefer, G.** (2001) Early diagenesis of organic matter from sediments off the eastern subtropical Atlantic: evidence from stable nitrogen and carbon isotopes. *Geochim. Cosmochim. Acta*, **65**, 1795–1808.

Fry, B., **Silva, S.R.**, **Kendall, C.** and **Anderson, R.K.** (2002) Oxygen isotope corrections for online $\delta(34)S$ analysis. *Rapid Commun. Mass Spectrom.*, **16**, 854–858.

Galli, M.T., **Jadoul, F.**, **Bernasconi, S.M.** and **Weissert, H.** (2005) Anomalies in global carbon cycling and extinction at the Triassic/Jurassic boundary: evidence from a marine C-isotope record. *Palaeogeogr. Palaeoclimatol. Palaeoecol.*, **216**, 203–214.

Gill, B.C., **Lyons, T.W.** and **Saltzman, M.R.** (2007) Parallel, high-resolution carbon and sulphur isotope records of the evolving Palaeozoic marine sulphur reservoir. *Palaeogeogr. Palaeoclimatol. Palaeoecol.*, **256**, 156–173.

Gill, B.C., **Lyons, T.W.** and **Frank, T.D.** (2008) Behavior of carbonate-associated sulfate during meteoric diagenesis and implications for the sulfur isotope palaeoproxy. *Geochim. Cosmochim. Acta*, **72**, 4699–4711.

Gill, B.C., **Lyons, T.W.**, **Young, S.A.**, **Kump, L.R.**, **Knoll, A.H.** and **Saltzman, M.R.** (2011) Geochemical evidence for widespread euxinia in the later Cambrian ocean. *Nature*, **469**, 80–83.

Gradstein, F.M., **Ogg, J.G.**, **Smith, A.G.**, **Bleeker, W.** and **Lourens, L.J.** (2004) A new Geologic Time Scale, with special reference to Precambrian and Neogene. *Episodes*, **27**, 83–100.

Gutschick, C.R. and **Sandberg, C.** (1983) Mississippian continental margins of the conterminous United States. In: *The Shelfbreak: Critical Interface on Continental Margins* (Eds. D.J. Stanley and G.T. Moore), Tulsa, Ok, *SEPM Spec. Publ., **33**, 79–96.*

Gutschick, R., **Sandberg, C.** and **Sando, W.** (1980) Mississippian shelf margin and carbonate platform from Montana to Nevada. *Paleozoic Paleogeography of the West-Central United States: Rocky Mountain Paleogeography Symposium*, **6**, 111–128.

Halverson, G.P., **Hoffman, P.F.**, **Schrag, D.P.** and **Kaufman, A.J.** (2002) A major perturbation of the carbon cycle before the Ghaub glaciation (Neoproterozoic) in Namibia: Prelude to snowball Earth? *Geochem. Geophys. Geosyst.*, **3**, 1–24.

Hatch, J.R. and **Leventhal, J.S.** (1997) Early diagenetic partial oxidation of organic matter and sulfides in the Middle Pennsylvanian (Desmoinesian) Excell Shale Member of the Fort Scott Limestone and equivalents, northern Midcontinent region, USA. *Chem. Geol.*, **134**, 215–235.

Hayes, J., **Strauss, H.** and **Kaufman, A.** (1999) The abundance of ^{13}C in marine organic matter and isotopic fractionation in the global biogeochemical cycle of carbon during the past 800 Ma. *Chem. Geol.*, **161**, 103–125.

Hoffman, P.F., **Kaufman, A.J.**, **Halverson, G.P.** and **Schrag, D.P.** (1998) A neoproterozoic snowball earth. *Science*, **281**, 1342–1346.

Huguet, C., **de Lange, G.J.**, **Gustafsson, Ö.**, **Middelburg, J.J.**, **Sinninghe Damsté, J.S.** and **Schouten, S.** (2008) Selective preservation of soil organic matter in oxidized marine

sediments (Madeira Abyssal Plain). *Geochim. Cosmochim. Acta*, **72**, 6061–6068.

Igamberdiev, A.U. and **Lea, P.J.** (2006) Land plants equilibrate O_2 and CO_2 concentrations in the atmosphere. *Photosynth. Res.*, **87**, 1–19.

Immenhauser, A., **Della Porta, G.**, **Kenter, J.A.M.** and **Bahamonde, J.R.** (2003) An alternative model for positive shifts in shallow-marine carbonate $\delta^{13}C$ and $\delta^{18}O$. *Sedimentology*, **50**, 953–959.

Immenhauser, A., **Holmden, C.** and **Patterson, W.** (2008) Interpreting the carbon-isotope record of ancient shallow epeiric seas: lessons from the Recent. In: *Dynamics of Epeiric Seas* (Eds B.R. Pratt and C. Holmden), Geological Association of Canada, Special Paper, **48**, 137–174.

Jenkyns, H.C. (2010) Geochemistry of oceanic anoxic events. *Geochem. Geophys. Geosyst.*, **11**, 1–30.

Johnson, E.A. (1992) Depositional history of Jurassic Rocks in the area of the Powder River Basin, Northeastern Wyoming and Southeastern Montana. *Bull. US Geol. Surv.*, **1917**, 1–319.

Johnston, D.T., **Macdonald, F.A.**, **Gill, B.C.**, **Hoffman, P.F.** and **Schrag, D.P.** (2012) Uncovering the Neoproterozoic carbon cycle. *Nature*, **483**, 320–324.

Jones, D.S. and **Fike, D.A.** (2013) Dynamic sulfur and carbon cycling through the end-Ordovician extinction revealed by paired sulfate-pyrite $\delta^{34}S$. *Earth Planet. Sci. Lett.*, **363**, 144–155.

Kampschulte, A., **Bruckschen, P.** and **Strauss, H.** (2001) The Sulphur isotopic composition of trace sulphates in Carboniferous brachiopods: implications for coeval seawater, correlation with other geochemical cycles and isotope stratigraphy. *Chem. Geol.*, **175**, 149–173.

Katz, D.A. (2008) Early and late diagenetic processes of Mississippian carbonates, northern US Rockies. PhD Dissertation, University of Miami, Coral Gables, FL, 444 pp. Available at: https://scholarlyrepository.miami.edu/oa_dissertations/154.

Katz, D.A., **Buoniconti, M.R.**, **Montanez, I.P.**, **Swart, P.K.**, **Eberli, G.P.** and **Smith, L.B., Jr** (2007) Timing and local perturbations to the carbon pool in the lower Mississippian Madison Limestone, Montana and Wyoming. *Palaeogeogr. Palaeoclimatol. Palaeoecol.*, **256**, 231–253.

Kaufman, A.J. and **Knoll, A.H.** (1995) Neoproterozoic variations in the C-isotopic composition of seawater: stratigraphic and biogeochemical implications. *Precambr. Res.*, **73**, 27–49.

Knoll, A.H., **Hayes, J.M.**, **Kaufman, A.J.**, **Swett, K.** and **Lambert, I.B.** (1986) Secular variation in carbon isotope ratios from Upper Proterozoic successions of Svalbard and East Greenland. *Nature*, **321**, 832–838.

Koch, J.T., **Frank, T.D.** and **Bulling, T.P.** (2014) Stable Isotope chemostratigraphy as a tool to correlate complex Mississippian marine carbonate facies of the Anadarko Shelf, Oklahoma-Kansas, USA. *AAPG Bull.*, **98**, 1071–1090.

Koevoets, M.J., **Abay, T.B.**, **Hammer, O.** and **Olaussen, S.** (2016) High-resolution organic carbon-isotope stratigraphy of the Middle Jurassic-Lower Cretaceous Agardhfjellet Formation of central Spitsbergen, Svalbard. *Palaeogeogr. Palaeoclimatol. Palaeoecol.*, **449**, 266–274.

Korte, C. and **Kozur, H.W.** (2010) Carbon-isotope stratigraphy across the Permian-Triassic boundary: A review. *J. Asian Earth Sci.*, **39**, 215–235.

Krull, E.S., **Lehrmann, D.J.**, **Druke, D.**, **Kessel, B.**, **Yu, Y.** and **Li, R.** (2004) Stable carbon isotope stratigraphy across the Permian-Triassic boundary in shallow marine carbonate platforms, Nanpanjiang Basin, south China. *Palaeogeogr. Palaeoclimatol. Palaeoecol.*, **204**, 297–315.

Kump, L.R. and **Garrels, R.M.** (1986) Modeling atmospheric O_2 in the global sedimentary redox cycle. *Am. J. Sci.*, **286**, 337–360.

Lamb, A.L., **Wilson, G.P.** and **Leng, M.J.** (2006) A review of coastal palaeoclimate and relative sea-level reconstructions using $\delta^{13}C$ and C/N ratios in organic material. *Earth Sci. Rev.*, **75**, 29–57.

Lane, H.R. and **Brenckle, P.L.** (2001) Type Mississippian subdivisions and biostratigraphic succession. In: *Stratigraphy and Biostratigraphy of the Mississippian Subsystem (Carboniferous System) in its Type Region, the Mississippi River Valley of Illinois, Missouri, and Iowa* (Ed. P.H. Heckel), I.U.G.S. Subcommission on Carboniferous Stratigraphy, Guidebook for Field Conference, St. Louis, MO, 83–107.

LaPorte, D.F., **Holmden, C.**, **Patterson, W.P.**, **Loxton, J.D.**, **Melchin, M.J.**, **Mitchell, C.E.**, **Finney, S.C.** and **Sheets, H.D.** (2009) Local and global perspectives on carbon and nitrogen cycling during the Hirnantian glaciation. *Palaeogeogr. Palaeoclimatol. Palaeoecol.*, **276**, 182–195.

Lee, C., **Fike, D.A.**, **Love, G.D.**, **Sessions, A.L.**, **Grotzinger, J.P.**, **Summons, R.E.** and **Fischer, W.W.** (2013) Carbon isotopes and lipid biomarkers from organic-rich facies of the Shuram Formation, Sultanate of Oman. *Geobiology*, **5**, 406–419.

Lehmann, M.F., **Bernasconi, S.M.**, **Barbieri, A.** and **Mckenzie, J.A.** (2002) Preservation of organic matter and alteration of its carbon and nitrogen isotope composition during simulated and in situ early sedimentary diagenesis. *Geochim. Cosmochim. Acta*, **66**, 3573–3584.

Luo, G., **Kump, L.R.**, **Wang, Y.**, **Tong, J.**, **Arthur, M.A.**, **Yang, H.**, **Huang, J.**, **Yin, H.** and **Xie, S.** (2010) Isotopic evidence for an anomalously low oceanic sulphate concentration following end-Permian mass extinction. *Earth Planet. Sci. Lett.*, **300**, 101–111.

Maughan, M. (1983) Tectonic setting of the Rocky Mountain region during the Late Palaeozoic and Early Mesozoic. In: *Proceedings of Symposium on the Genesis of Rocky Mountain Ore Deposits: Changes with Time and Tectonics*. pp. 39–50. Denver Regional Exploration Geologists Society.

Meyer, K.M., **Yu, M.**, **Jost, A.B.**, **Kelley, B.M.** and **Payne, J.L.** (2011) $\delta^{13}C$ evidence that high primary productivity delayed recovery from end-Permian mass extinction. *Earth Planet. Sci. Lett.*, **302**, 378–384.

Meyer, K.M., **Yu, M.**, **Lehrmann, D.**, **van de Schootbrugge, B.** and **Payne, J.L.** (2013) Constraints on Early Triassic carbon cycle dynamics from paired organic and inorganic carbon isotope records. *Earth Planet. Sci. Lett.*, **361**, 429–435.

Mii, H., **Grossman, E.** and **Yancey, T.** (1999) Carboniferous isotope stratigraphies of North America: Implications for Carboniferous palaeoceanography and Mississippian glaciation. *Geol. Soc. Am. Bull.*, **111**, 960–973.

Millward, D., **Davies, S.J.**, **Williamson, F.**, **Curtis, R.**, **Kearsey, T.I.**, **Bennet, C.E.**, **Marshall, J.E.A.** and **Browne, M.A.E.** (2018) Early Mississippian evaporites of coastal tropical wetlands. *Sedimentology*, https://doi.org/10.1111/sed.12465.

Nunn, E.V., **Price, G.D.**, **Hart, M.B.**, **Page, K.N.** and **Leng, M.J.** (2009) Isotopic signals from Callovian-Kimmeridgian (Middle-Upper Jurassic) belemnites and bulk organic carbon, Staffin Bay, Isle of Skye, Scotland. *J. Geol. Soc.*, **166**, 633–641.

Oehlert, A.M. and **Swart, P.K.** (2014) Interpreting carbonate and organic carbon isotope covariance in the sedimentary record. *Nat. Commun.*, **5**, 4672.

Oehlert, A.M., **Lamb-Wozniak, K.A.**, **Devlin, Q.B.**, **Mackenzie, G.J.**, **Reijmer, J.J.G.** and **Swart, P.K.** (2012) The stable carbon isotopic composition of organic material in platform derived sediments: implications for reconstructing the global carbon cycle. *Sedimentology*, **59**, 319–335.

Peters-Kottig, W., **Strauss, H.** and **Kerp, H.** (2006) The land plant $\delta^{13}C$ record and plant evolution in the Late Palaeozoic. *Palaeogeogr. Palaeoclimatol. Palaeoecol.*, **240**, 237–252.

Prahl, F.G., **De Lange, G.J.**, **Scholten, S.** and **Cowie, G.L.** (1997) A case of post-depositional aerobic degradation of terrestrial organic matter in turbidite deposits from the Madeira Abyssal Plain. *Org. Geochem.*, **27**, 141–152.

Saltzman, M. (2002) Oxygen isotope stratigraphy of the Lower Mississippian (Kinderhookian–lower Osagean), western United States: implications for seawater chemistry and glaciation. *Geol. Soc. Am. Bull.*, **114**, 96–108.

Saltzman, M.R. (2003) Organic Carbon Burial and Phosphogenesis in the Antler Foreland Basin: An out-of-phase relationship during the Lower Mississippian. *J. Sediment. Res.*, **73**, 844–855.

Saltzman, M.R., **Groessens, E.** and **Zhuravlev, A.V.** (2004) Carbon cycle models based on extreme changes in $\delta^{13}C$: an example from the lower Mississippian. *Palaeogeogr. Palaeoclimatol. Palaeoecol.*, **213**, 359–377.

Saltzman, M.R., **Ripperdan, R.L.**, **Brasier, M.D.**, **Lohmann, K.C.**, **Robison, R.A.**, **Chang, W.T.**, **Peng, S.-C.**, **Ergaliev, E.K.** and **Runnegar, B.** (2000) A global carbon isotope excursion (SPICE) during the Late Cambrian: relation to trilobite extinctions, organic-matter burial and sea level. *Palaeogeogr. Palaeoclimatol. Palaeoecol.*, **162**, 211–223.

Sando, W. (1977) Stratigraphy of the Madison Group (Mississippian) in the northern part of the Wyoming-Idaho Overthrust Belt and adjacent areas. *Wyoming Geological Association 29th Annual Field Conference Guidebook*, pp. 173–177.

Sando, W. (1985) Revised Mississippian time scale, western interior region, conterminous United States. *U.S. Geol. Surv. Bull.*, **1605-A**, A15–A26.

Sando, W.J. and **Bamber, E.W.** (1985) Coral zonation of the Mississippian system in the Western Interior Province of North America. *US Geol. Surv. Prof. Pap.*, **1334**, 1–61.

Sando, W.J., **Mamet, B.L.** and **Dutro.Jr, J.T.** (1969) Carboniferous megafaunal and macrofaunal zonation of the Northern Cordillera of the United States. *Contributions to Paleontology, U.S. Geological Survey Professional Paper*, **613-E, 29**, E1–E25.

Scotese, C.R. and **McKerrow, W.S.** (1990) Revised World maps and introduction. *Geol. Soc. London Mem.*, **12**, 1–21.

Smith, L., Jr, **Eberli, G.P.** and **Sonnenfeld, M.** (2004) Sequence-stratigraphic and Palaeogeographic distribution of reservoir-quality dolomite, Madison Formation, Wyoming and Montana. Integration of outcrop and modern analogs in reservoir modeling. *AAPG Mem.*, **80**, 67–92.

Sonnenfeld, M. (1996) Sequence evolution and hierarchy within the lower Mississippian Madison limestone of Wyoming. In: *Palaeozoic Systems of the Rocky Mountain Region* (Eds M.W. Longman and M.D. Sonnenfeld), pp. 165–192. Rocky Mountain Section SEPM – Society for Sedimentary Geology, Denver, CO.

Strauss, H. and **Peters-Kottig, W.** (2003) The Paleozoic to Mesozoic carbon cycle revisited: The carbon isotopic composition of terrestrial organic matter. *Geochem. Geophys. Geosyst.*, **4**, 1–15.

Swanson-Hysell, N.L., **Rose, C.V.**, **Calmet, C.C.**, **Halverson, G.P.**, **Hurtgen, M.T.** and **Maloof, A.C.** (2010) Cryogenian glaciation and the onset of carbon-isotope decoupling. *Science*, **328**, 608–611.

Swart, P.K. (2008) Global synchronous changes in the carbon isotopic composition of carbonate sediments unrelated to changes in the global carbon cycle. *Proc. Natl Acad. Sci. USA*, **105**, 13741–13745.

Swart, P.K. and **Eberli, G.P.** (2005) The nature of the $\delta^{13}C$ of periplatform sediments: Implications for stratigraphy and the global carbon cycle. *Sed. Geol.*, **175**, 115–129.

Swart, P.K. and **Oehlert, A.M.** (2018) Revised interpretations of stable C and O patterns in carbonate rocks resulting from meteoric diagenesis. *Sed. Geol.*, **364**, 14–23.

Turchyn, A.V. and **Schrag, D.P.** (2004) Oxygen isotope constraints on the sulfur cycle over the past 10 million years. *Science*, **303**, 2004–2007.

Veevers, J.J. and **Powell, C.M.** (1987) Late Paleozoic glacial episodes in Gondwanaland reflected in transgressive-regressive depositional sequences in Euramerica. *Geol. Soc. Am. Bull.*, **98**, 475–487.

Walker, J.C.G. (1986) Global geochemical cycles of carbon, sulfur, and oxygen. *Mar. Geol.*, **70**, 159–174.

Wang, X., **Jiang, G.**, **Shi, X.** and **Xiao, S.** (2016) Paired carbonate and organic carbon isotope variations of the Ediacaran Doushantuo Formation from an upper slope section at Siduping, South China. *Precambr. Res.*, **273**, 53–66.

Werne, J.P. and **Hollander, D.J.** (2004) Balancing supply and demand: controls on carbon isotope fractionation in the Cariaco Basin (Venezuela) Younger Dryas to present. *Mar. Chem.*, **92**, 275–293.

Westphal, H., **Eberli, G.P.**, **Smith, L.B.**, **Grammer, G.M.** and **Kislak, J.** (2004) Reservoir characterization of the Mississippian Madison Formation, Wind River basin, Wyoming. *AAPG Bull.*, **4**, 405–432.

Young, S.A., **Saltzman, M.R.**, **Bergstrom, S.M.**, **Lesli, S.A.** and **Xu, C.** (2008) Paired $\delta^{13}C_{carb}$ and $\delta^{13}C_{org}$ records of Upper Ordovician (Sandbian-Katian) carbonates in North America and China: Implications for Palaeoceanographic change. *Palaeogeogr. Palaeoclimatol. Palaeoecol.*, **270**, 703–714.

Manuscript received 21 July 2017; revision accepted 1 June 2018